AD-A038 888 TRW SYSTEMS GROUP REDONDO BEACH CALIF F/G 21/2
ON DIFFUSION FLAMES IN TURBULENT SHEAR FLOWS: MODELING REACTANT--ETC(U)
1977 W B BUSH, P S FELDMAN, F E FENDELL DAAG29-74-C-0023
UNCLASSIFIED ARO-11674.5-E NL

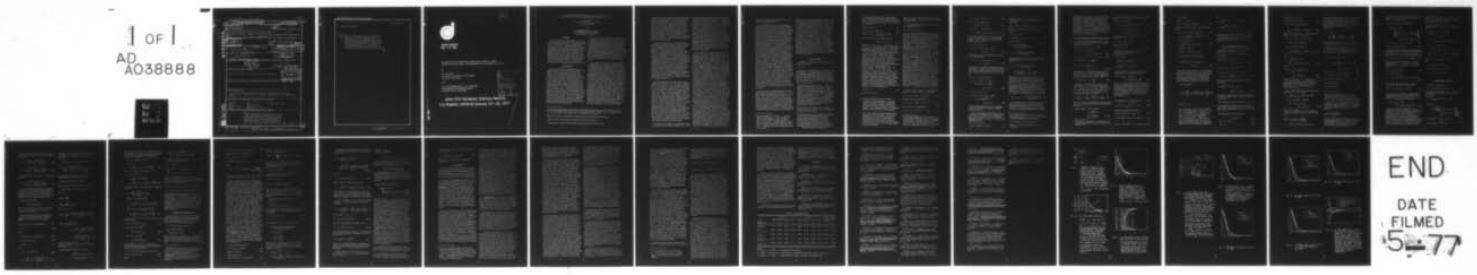

Unclassified

SECURITY CLASSIFICATION OF THIS PAGE (When Data Entered)

REPORT DOCUMENTATION PAGE

READ INSTRUCTIONS BEFORE COMPLETING FORM

1. REPORT NUMBER: ARO 11674.5-E	2. GOVT ACCESSION NO.
3. RECIPIENT'S CATALOG NUMBER	
4. TITLE (and Subtitle): ON DIFFUSION FLAMES IN TURBULENT SHEAR FLOWS: MODELING REACTANT CONSUMPTION IN A PLANAR FUEL JET.	5. TYPE OF REPORT & PERIOD COVERED: Reprint
	6. PERFORMING ORG. REPORT NUMBER
7. AUTHOR(s): W. B. Bush, P. S. Feldman, F. E. Fendell	8. CONTRACT OR GRANT NUMBER(s): DAAG29-74-C-0023, new
9. PERFORMING ORGANIZATION NAME AND ADDRESS: TRW Systems Group, Redondo Beach, California 354595	10. PROGRAM ELEMENT, PROJECT, TASK AREA & WORK UNIT NUMBERS: NSF-ENG-74-11828
11. CONTROLLING OFFICE NAME AND ADDRESS: U. S. Army Research Office, Post Office Box 12211, Research Triangle Park, NC 27709	12. REPORT DATE: 11 1977
	13. NUMBER OF PAGES: 22
14. MONITORING AGENCY NAME & ADDRESS (if different from Controlling Office): 12 25p.	15. SECURITY CLASS. (of this report): Unclassified
	15a. DECLASSIFICATION/DOWNGRADING SCHEDULE

16. DISTRIBUTION STATEMENT (of this Report)

Approved for public release; distribution unlimited.

DDC RECEIVED APR 29 1977 A

17. DISTRIBUTION STATEMENT (of the abstract entered in Block 20, if different from Report)

18. SUPPLEMENTARY NOTES

The findings in this report are not to be construed as an official Department of the Army position, unless so designated by other authorized documents.

19. KEY WORDS (Continue on reverse side if necessary and identify by block number)

Diffusion	Jets	Mathematical models
Flames	Subsonic flow	
Turbulent flow	Chemical reactions	
Fuels	Oxidizers	

20. ABSTRACT (Continue on reverse side if necessary and identify by block number)

The turbulent portion of the planar fuel jet, for isobaric subsonic flow, under fast direct one-step irreversible reaction between unpremixed fuel and oxidant, is analyzed. Mean spatial profiles for the dependent variables are found numerically and analytically from the governing nonlinear partial → next page

DD FORM 1 JAN 73 1473 EDITION OF 1 NOV 65 IS OBSOLETE

354595

Unclassified

SECURITY CLASSIFICATION OF THIS PAGE (When Data Entered)

ARO 11674.5-E

20. ABSTRACT CONTINUED

cont

differential equations, based on an explicit eddy diffusion, and on a mean rate of reactant consumption proportional to the product of the mean mass fraction of fuel, the mean mass fraction of oxidant, and the appropriate local characterization of the mean rate of strain. Results from the model are qualitatively, and, in many cases, quantitatively, compatible with experimental data.

AIAA PAPER
NO. 77-96

ON DIFFUSION FLAMES IN TURBULENT SHEAR FLOWS: MODELING REACTANT CONSUMPTION IN A PLANAR FUEL JET

by

W. B. BUSH
University of California, San Diego
La Jolla, California

and

P. S. FELDMAN and F. E. FENDELL
TRW Systems and Energy Group
Redondo Beach, California

AIAA 15th Aerospace Sciences Meeting
Los Angeles, California/January 24-26, 1977

ON DIFFUSION FLAMES IN TURBULENT SHEAR FLOWS: MODELING REACTANT CONSUMPTION IN A PLANAR FUEL JET*

W. B. Bush**
University of California, San Diego
La Jolla, California

and

P. S. Feldman† and F. E. Fendell‡
TRW Systems and Energy Group
Redondo Beach, California

Abstract

The turbulent portion of the planar fuel jet, for isobaric subsonic flow, under fast direct one-step irreversible reaction between unpremixed fuel and oxidant, is analyzed. Mean spatial profiles for the dependent variables are found numerically and analytically from the governing nonlinear partial differential equations, based on an explicit eddy diffusion, and on a mean rate of reactant consumption proportional to the product of the mean mass fraction of fuel, the mean mass fraction of oxidant, and the appropriate local characterization of the mean rate of strain. Results from the model are qualitatively, and, in many cases, quantitatively, compatible with experimental data.

I. Introduction

In many aerothermochemical devices, the rapid burning of initially unmixed, but highly combustible, gases is preferred for control and safety. The essential point is that the rate of consumption of reactants, and the generation of products and of chemical exothermicity are usually controlled by unsteady, inviscid, inertial, large-scale mixing. Once the large-scale structure is broken down (to permit molecularly controlled small-scale mixing and chemical mechanisms to proceed), the formation of product gas occurs rapidly. In fact, to keep such devices to practical dimensions, the intuitively faster mixing associated with unsteady, turbulent diffusion, as opposed to laminar diffusion, is preferred. (Hence, if the flow is not naturally unsteady, transition is often artificially induced.) Thus, the combustion of unpremixed gases in turbulent shear flows, or (more succinctly) turbulent diffusion flames, remains one of the subjects in aerothermochemistry and most worthy of intense study.

Of course, not all turbulent reacting flows fall into the category of turbulent diffusion flames, and, in these other cases, more general approaches (retaining the roles of finite-rate chemical kinetics and of molecular-scale mixing, as well as that of large-scale turbulent diffusion) are necessary. It is intriguing for modelers to attempt these more complicated cases, but, from a practical point-of-view, turbulent diffusion flames remain one of the most recurrent phenomena in combustion. If so practically important and relatively simple a problem cannot be feasibly treated, then, the outlook for the treatment of these more difficult cases dims.

The present work is also motivated by what the authors believe to be a realistic appraisal of (1) design needs; (2) available experimental data to serve as boundary/initial conditions to initiate a prediction, and as comparisons to validate such a prediction; and (3) current physical understanding of turbulent transfer. A relatively rapid and inexpensive means of explicitly characterizing the alteration in system performance as a function of alteration in controllable parameters is often what is primarily sought by the designer. Properties of the turbulence are often not of as much practical interest as behaviors of the dependent variables, themselves. In fact, properties of the turbulence are usually not known, and must be arbitrarily adopted at initial and/or boundary stations in computations involving higher-order closures. Where sensitivity to such assumptions dissipates, the flow may well be close enough to local turbulent equilibrium that explicit lower-order closures are adequate. Another problem with such higher-order closures is that the conceptually systematic developments become ultimately vitiated in practice, because of the need to adopt relatively arbitrary statements concerning the integral

*This work was supported by the National Science Foundation under grant ENG 74-11828 and by the U.S. Army Research Office under contract DAAG29 74 C 0023. The advice and encouragement of Dr. G. F. Carrier, Harvard University, are gratefully acknowledged.

**Research Engineer, Department of Applied Mechanics and Engineering Sciences.

†Member of the Technical Staff, Engineering Sciences Laboratory.

‡Staff Engineer, Engineering Sciences Laboratory; Associate Fellow, AIAA.

length scale of the turbulence and/or the functional forms of the probability distribution functions for the dependent variables. Unless consistency in the level of approximation of a coupled nonlinear system is maintained, professions of accuracy become moot. Thus, intricate formulation necessarily incurs additional expense, but does not necessarily achieve additional validity. In an almost inevitably semi-empirical subject as turbulent reacting shear flows, the simplest formulation, adequate in terms of available data and engineering design for a particular, yet commonly occurring, case, i.e., turbulent diffusion flames, appears worth identifying.

Of special interest here is the application of modeling of unsteady diffusion flames to diffusion-type continuous chemical lasers, in which highly dissociated fluorine reacts with bimolecular hydrogen (or deuterium) to form an activated product. For this particular case, a direct one-step irreversible chemical reaction is the actual chemical mechanism, not a simulation (Kerber, Emanuel and Whittier[1]). Chemical lasers operable at higher cavity pressure levels are of interest; such higher levels still leave three-body reactions negligibly slow relative to the two-body mechanism. While higher pressure increases the degree of unsteadiness in the flow field, the Reynolds numbers are small enough that conventional concepts of fully-developed turbulence do not apply to the pumping. In fact, consideration of the large-scale structure recently emphasized in transitional and unsteady shear flow is doubtlessly relevant (Davies and Yule[2]; Roshko[3]). Modifications of the large-scale structure at higher Reynolds numbers do not appear pertinent.

For such large-scale structure, both a local instantaneous theory for unsteady diffusion flames (Bush and Fendell[4]; Carrier, Fendell and Marble[5]; Carrier and Fendell[6]), and also a mean theory for the time-averaged description (Bush and Fendell[7,8]; Bush, Feldman and Fendell[9]) have appeared in the literature. The model is particularly suitable for those cases, such as hydrogen-fluorine cold-step chemistry, in which the first Damköhler number is large, so that, instantaneously, a thin flame arises. (Large first Damköhler number implies that the reaction rate is large relative to the flow rate, so that the aerothermochemical system is in, or very close to, chemical equilibrium.) In such cases, in time-average, the mean rate of reactant consumption is taken to be related to the product of the mean mass fraction of oxidant, the mean mass fraction of fuel, and the principal mean strain rate (for the parabolic formulation appropriate for the thin shear layers of interest here). It is argued that, in general, the magnitude of the principal mean strain rate indicates the level of local chemical activity in a turbulent diffusion flame in which macroscopic mixing is rate-controlling.

The explicit local algebraic (as opposed to field-type differential) expression adopted for the mean rate of chemical reaction is compatible with the adoption of an explicit local algebraic (eddy viscosity) expression for the mean rate of diffusive transport. It is believed that: (1) it is inconsistent to adopt a second-order closure for the mean kinetics or eddy transport, and an explicit (or first-order) closure for the other; (2) it is premature to examine second-order closure for either the mean kinetics or the mean diffusive transport until the local explicit algebraic relations, into which such formulations degenerate in local turbulent equilibrium, are first examined for plausibility; and (3) the additional complexity of second-order closures for nondefect-layer-type flow geometries (Spalding[10,11]; Ooms and Wicks[12]; Spalding[13]) has not been justified by proof of sufficient additional validity in prediction, and, for defect-layer-type geometries, explicit closures are quite competitive with second-order closures (Reynolds[14]).

The present model has been studied in detail for the mixing layer formed by two parallel streams, a geometry of interest towards the end of the lasing zone in a diffusion-type continuous chemical laser cavity (Bush, Feldman and Fendell[9]). However, whereas the fully-developed mixing layer is tractable for analysts, it is difficult for experimentalists, and, thus, some empirical constants in the theory remain unassigned for lack of data. Experimentalists have treated the fuel jet exhausting into an oxidant-containing ambient (e.g., Hawthorne, Weddell and Hottel[15]; Kremer[16]; Kent and Bilger[17]; Bilger and Beck[18]), and, under the assumption that values for empirical factors are transferrable between the geometries, a solution is sought here for the two-dimensional fuel jet. The major new feature introduced by the fuel jet, without counterpart in the (downstream) mixing layer, is the plane of antisymmetry for the principal mean strain rate (henceforth referred to as a line of symmetry, since a transverse cross-section only needs to be considered). Because the mean strain rate is odd about the axis, clearly, it is the magnitude of the strain rate that is relevant for modeling the mean consumption rate. The question has been raised as to whether a model giving zero reaction rate at the axis can be used to describe measured properties of turbulent jet (or wake) flows with diffusion flames (Williams[19]), and this point is to be resolved below. Because this work is motivated by interest in pumping phenomena in the cavity of a diffusion-type continuous chemical laser, as noted earlier, this question definitely warrants an answer: the upstream end of the pumping zone has wake-like character that evolves into mixing-layer-like character only towards the downstream end of the pumping zone in chemical lasers (Grohs[20]). Capacity of the model to treat a turbulent diffusion flame for the planar-jet configuration, with its plane of antisymmetry for the principal mean strain rate, and to treat such a flame for the mixing-layer configuration, with its plane of symmetry, suggests that the model

can treat the turbulent diffusion flame for a wake evolving into a mixing layer.

It is worthwhile to recall some well-known properties of turbulent jets, in order to delineate the portion of the flow field of pertinence here. When fluid emerges from a nozzle into the stagnant ambient, marginally unstable mixing layers form at the lips of the nozzle, and, eventually, merge on the plane of symmetry, where the constant-velocity, constant-thermodynamic-property 'potential core' terminates (Fig. 1). This distance is on the order of six nozzle widths downstream (Beer and Chigier[21]; Davies[22]), and methods for calculating this distance have been advanced (Lessen and Paillet[23]). This distance from the exit is sometimes referred to as the 'breakpoint', because the jet begins spreading at a greater rate from this distance downstream. Actually, even after this merger distance, an (additional) distance of several nozzle widths is required before the transitional flow becomes fully turbulent and, in the chemically frozen case, a fully-developed turbulence and self-similar representations of velocity, species, and temperature profiles become appropriate. It is common, since, in any transverse downstream plane, in the chemically frozen case, the flux of momentum, of discharged fluid, and of discharged enthalpy above ambient are invariant, to treat the jet as if it were emitted from an ideal source, rather than from a nozzle of finite dimension. Since the interest here is in chemically reacting flows, source ideas are modified as convenient. In fact, in effect, it is taken below that initial profiles for the dependent variables are given at the 'breakpoint'. In the absence of data, plausible interpolations between nozzle properties, which hold at the axis at the merger point, and ambient values, which hold far from the axis at all downstream distances, are to be adopted.

There are three observations about the model just presented that warrant discussion. (1) It is being implicitly assumed that the distance to transition is also approximately the distance to initiation of burning. This model is conventional,* and jet diffusion flames are commonly described as 'lifted', because they stand off a finite distance from the nozzle exit. Attempts to describe this stand-off regime in detail inevitably entail arbitrary assumptions, the validity of which are difficult to evaluate (Tamanini[25]). (2) Although more experimental data are available for axisymmetric turbulent jet diffusion flames than for planar turbulent jet diffusion flames, the planar case is being developed here for two reasons. One is that existing diffusion-type continuous chemical lasers, ultimately motivating this work, involve a planar geometry. The other reason is that, for simplicity, a self-similar representation of the flow field is employed, in order not to complicate the energetics, which is of prime concern. Such a self-similar representation has a greater domain of validity for the planar jet than for the axisymmetric jet.* (3) The linear rate of planar jet growth with downstream distance, postulated by self-similar analysis for the fully-developed turbulent flow, has been questioned recently as perhaps slightly in error far downstream (Kotsovinos[27]).** Even if such a discrepancy does exist, both the magnitude of the effect, and the fact that distances far downstream of the flame-tip length are of less interest make this observation of little significance for present purposes.

II. Formulation

The direct one-step irreversible bimolecular chemical reaction

$$F + O \rightarrow P, \qquad (1)$$

in which fuel F and oxidant O yield product P, is considered. The flow geometry studied is that of a low-speed symmetric planar jet of one reactant (say, fuel) exhausting into a stagnant atmosphere containing the other reactant. In the limit of (1) $\underline{R} = \rho_r u_r \ell_r / \mu_r$, the (reference) Reynolds number, going to infinity,*** and (2) $\underline{M} = u_r / (\gamma R T_r)^{\frac{1}{2}}$,

---

*Wohl and Shipman[24] comment: "... there is always some distance ... above the port for which the flame appears free of turbulence. Since, in that region, mixing probably occurs by molecular diffusion, and since molecular diffusion is a slower mixing process than eddy diffusion, it is assumed that little combustion occurs in this region."

*Gutmark and Wygnanski[26] remark: "The normalized turbulent intensities on the [center-] plane of the jet attain their self-preserving state about thirty slot widths downstream from the nozzle. ... The approach to self-preservation in a two-dimensional jet, thus, occurs much earlier than in an axisymmetric jet ... or a two-dimensional wake. In contrast to an axisymmetric jet, there is no indication here that the transverse and lateral components ... of the velocity fluctuations attain self-preservation long after the [streamwise] component does."

**This variance in the linear rate of growth is ascribed to the nature of the flow outside the jet induced by the jet, itself.

***Since the experiments of Hawthorne, Weddell and Hottel,[15] it has been established that the ratio of flame length (by any reasonable phenomenological definition) to initial jet radius is invariant with initial jet velocity in turbulent flow, to excellent approximation. In nondimensional terms, the ratio is invariant with Reynolds number, for Reynolds numbers

(footnote continued on next page)

the (reference) Mach number, going to zero, the (nondimensional) boundary-layer approximations* to the governing conservation equations for the time-averaged description of the turbulent reacting jet are:

$$(\rho u)_{,x} + (\rho v)_{,y} = 0; \tag{2}$$

$$\rho u u_{,x} + \rho v u_{,y} = (\rho \epsilon u_{,y})_{,y}; \tag{3}$$

$$\rho u T_{,x} + \rho v T_{,y} = \frac{1}{\sigma_h} (\rho \epsilon T_{,y})_{,y} + Q\dot{w}; \tag{4}$$

$$\rho u Y_{i,x} + \rho v Y_{i,y} = \frac{1}{\sigma_i} (\rho \epsilon Y_{i,y})_{,y} + \dot{w}_i,$$

$$\text{with } i = F, O, P. \tag{5}$$

Here, (1) $x = x_k/\ell_r$ and $y = y_k/\ell_r$, with $x \geq 0$, $0 \leq y < \infty$, are the streamwise and normal spatial coordinates, respectively, with ℓ_r = reference length (the initial jet width); (2) $u = u_k/u_r$ and $v = v_k/u_r$ are the mean streamwise and normal velocity components, respectively, with u_r = reference velocity (the initial jet velocity); (3) $\rho = \rho_k/\rho_r$ and $T = T_k/T_r$ are the mean density and (absolute) temperature of the mixture, respectively, with $\rho_r R T_r = p_r$, where p_r = reference pressure (the background and jet pressure); (4) Y_i is the mean (stoichiometrically adjusted) mass fraction of species i; (5) $Q = Q_k/c_p T_r$ is the specific heat of combustion; while $\dot{w}\ (= -\dot{w}_F = -\dot{w}_O = \dot{w}_P) = \dot{w}_k/(\rho_r u_r/\ell_r)$ is the mean rate of reactant consumption (and product generation); (6) $\epsilon = \epsilon_k/u_r \ell_r$ is the eddy viscosity (or turbulent momentum-diffusion coefficient); while σ_h and σ_i are the (constant) turbulent Prandtl number and turbulent Schmidt numbers for species i, respectively, such that ϵ/σ_h and ϵ/σ_i are the turbulent heat-conduction and species-diffusion coefficients. Further, in this formulation, the (nondimensional) equation of state is postulated to be:

$$p = \rho T = 1, \tag{6}$$

where $p = p_k/p_r$ is the mean pressure, and the molecular weights of all species present are taken as comparable.

In the analysis that follows, the mean reaction rate is postulated to be:

$$\dot{w} = (\rho \beta |u_{,y}|) Y_F Y_O, \tag{7}$$

where β is the (nondimensional) function* that characterizes the rate of chemical consumption relative to the rate of species transport. Because, for the case of predominant interest here, in which $y = 0$ is an axis of (even or odd) symmetry for all the dependent variables, the factor $u_{,y}$ is odd about $y = 0$, the expression for $\dot{w}$ is continuous at $y = 0$, but $\dot{w}_{,y}$ (and all higher derivatives) are discontinuous. The source of this difficulty is that, more generally, $|u_{,y}|$ is $\Phi^{\frac{1}{2}}$, where Φ is the velocity-gradient factor of the conventional laminar dissipation expression written in terms of the mean velocity field components. Whereas $|u_{,y}|$ is a satisfactory approximation to $\Phi^{\frac{1}{2}}$ throughout most of the flow field; near $y = 0$ (where $u_{,y} \to 0$), other discarded terms in $\Phi^{\frac{1}{2}}$ should be restored in the leading-order approximation for the local strain rate. For simplicity, a conventional parabolic formulation is adopted here, and, near $y = 0$, an even function of y, which recovers whatever degree of smoothness is believed important, may be 'patched' into the (elsewhere uniformly valid) expression for $|u_{,y}|$. The amount of chemical activity at the axis is believed to be of such magnitude, relative to the amount of chemical activity off the axis, over most of the axial positions of interest, and the nature of the experimental data for a reacting jet is such, that it is believed that adoption of (7) is currently acceptable on physical grounds. Thus, (7) is modified locally at $y = 0$ only as required analytically.

For $\underline{R} \to \infty$, $\underline{M} \to 0$, and $p = 1$, with the introduction of (1) the coordinate transformation

$$(x, y) \to (x, z), \quad \text{with } z = \int_0^y \left(\frac{1}{T}\right) dy', \tag{8a}$$

and (2) the velocity transformation

$$(u, v) \to (U, V), \quad \text{with } U = u,\ V = u z_{,x} + v z_{,y}, \tag{8b}$$

(2) - (7) may be re-expressed as:

$$U_{,x} + V_{,z} = 0: \quad U = \Psi_{,z}, \quad V = -\Psi_{,x}; \tag{9}$$

(footnote continued from previous page)

in excess of a couple thousand. This result infers that molecular diffusion is negligible relative to inviscid, inertial, macroscopic processes for gaseous turbulent jet diffusion flames. Thus, molecular diffusion is neglected relative to eddy diffusion in the formulation.

* Here, the boundary-layer approximations are invoked on an intuitive basis. That these approximations are valid ones is not at all a straightforward matter to demonstrate for turbulent flows. It must be proved experimentally (or otherwise) that any terms dropped from the equations are, in fact, small compared to the terms retained.

* A preliminary suggestion is that, in general, β is inversely proportional to $m = (\nu_F m_F + \nu_O m_O)$, where m_i and ν_i are the molecular weight and stoichiometric coefficient, respectively, of species i. Here, the case $\nu_O, \nu_F = 1$, $m_O, m_F \approx m_X$ is being examined, so that $m \approx 2m_X$.

$$UU_{,x} + VU_{,z} - (DU_{,z})_{,z} = 0; \qquad (10)$$

$$UT_{,x} + VT_{,z} - \frac{1}{\sigma_h}(DT_{,z})_{,z} = Q(B|U_{,z}|)\,Y_F Y_O; \qquad (11)$$

$$UY_{i,x} + VY_{i,z} - \frac{1}{\sigma_i}(DY_{i,z})_{,z} = -(B|U_{,z}|)\,Y_F Y_O, \text{ with } i = F, O. \qquad (12)$$

In the above equations, $D = \epsilon/T^2$ and $B = \beta/T$. For this system of equations, it is taken that stagnant uniform conditions characterize the ambient, specifically:

$$U \to U_\infty = 0,\ T \to T_\infty = 1,$$

$$Y_F \to Y_{F\infty} = 0,\ Y_O \to Y_{O\infty} = \text{const.}$$

$$\text{as } z \to \infty. \qquad (13)$$

For symmetric initial conditions, at the centerline, it is taken that

$$V \to 0,\ U_{,z},\ T_{,z},\ Y_{F,z},\ Y_{O,z} \to 0$$

$$\text{as } z \to 0. \qquad (14)$$

(Obviously, for the sake of specificity only, the jet is taken to contain fuel, but not oxidant; and the ambient is taken to contain oxidant, but not fuel.) The initial conditions at the jet exit plane are

$$U \to U_j = 1,\ T \to T_j = \text{const.} \geq 1,$$

$$Y_F \to Y_{Fj} = \text{const.},\ Y_O \to Y_{Oj} = 0$$

$$\text{for } 0 \leq z < z_j = \tfrac{1}{2}\left(\frac{1}{T_j}\right)$$

$$\text{as } x \to x_j = 0; \qquad (15a)$$

$$U \to U_\infty = 0,\ T \to T_\infty = 1,$$

$$Y_F \to Y_{F\infty} = 0,\ Y_O \to Y_{O\infty} = \text{const.}$$

$$\text{for } z_j = \tfrac{1}{2}\left(\frac{1}{T_j}\right) < z < \infty$$

$$\text{as } x \to x_j = 0. \qquad (15b)$$

The specified functions of (15) are compatible with (13), and with the requisite of initially unmixed reactants.

Since, experimentally (Batt[28]), $\sigma_h, \sigma_i \simeq \sigma$, it is convenient to introduce the (turbulent) Shvab-Zeldovich functions Φ_q, linear sums of the dependent variables T and Y_i. The functions adopted here are:

$$\Phi_Y = (Y_F - Y_O) \equiv Y;$$

$$\Phi_T = T + \tfrac{1}{2}Q(Y_F + Y_O) \equiv \epsilon. \qquad (16)$$

From (11) and (12), it is found that the conservation equations for these Shvab-Zeldovich functions are:

$$U\Phi_{q,x} + V\Phi_{q,z} - \frac{1}{\sigma}(D\Phi_{q,z})_{,z} = 0. \qquad (17)$$

Directly, it is seen that the following integral holds:

$$\epsilon = aY + b \text{ and/or}$$

$$T + \tfrac{1}{2}Q(Y_F + Y_O) = a(Y_F - Y_O) + b, \qquad (18a)$$

where, from (15),

$$a = \frac{(T_j - 1) + \tfrac{1}{2}Q(Y_{Fj} - Y_{O\infty})}{(Y_{Fj} + Y_{O\infty})},$$

$$b = 1 + \frac{(T_j - 1)Y_{O\infty} + QY_{Fj}Y_{O\infty}}{(Y_{Fj} + Y_{O\infty})}. \qquad (18b)$$

It is noted that (18) can be rewritten to yield the following expression for T as a function of Y_F and Y_O:

$$T = 1 + \frac{(T_j - 1)\left(Y_F + (Y_{O\infty} - Y_O)\right)}{(Y_{Fj} + Y_{O\infty})} + \frac{Q\,Y_{Fj}Y_{O\infty}}{(Y_{Fj} + Y_{O\infty})}\left(1 - \frac{Y_F}{Y_{Fj}} - \frac{Y_O}{Y_{O\infty}}\right). \qquad (19)$$

Physically, $Y_F \leq Y_{Fj}$ and $Y_O \leq Y_{O\infty}$. Thus, if the (so-called) adiabatic flame temperature (defined to be the temperature achieved where both Y_O and Y_F are zero) is denoted by T_{af}, then T_{af} is the maximum temperature achievable in the flow system. Since, experimentally (Hawthorne, Weddell and Hottel[15]; Kent and Bilger[17]), it is known that the turbulent diffusion flame has finite mean structure, i.e., Y_O and Y_F never vanish simultaneously, it follows that

$$1 \leq T < T_{af} = b = 1 + \frac{(T_j - 1)Y_{O\infty} + QY_{Fj}Y_{O\infty}}{(Y_{Fj} + Y_{O\infty})}. \qquad (20)^*$$

It is noted that, even with the obtaining of the above integral relating the Shvab-Zeldovich functions, the dynamics ((9) and (10)) and energetics ((11) and (12)) remain coupled. In general, D and B, the turbulent diffusion and reaction

---

*If an effective flame position for the turbulent flow is defined by the locus $Y_O = Y_F \equiv X_f$, then, the flame temperature T_f is given by

$$T_f = T_{af} - QX_f : (T_{af} - T_f) = QX_f > 0,$$

where T_f and X_f are, in general, not constants.

coefficients, respectively, are functions of the temperature (and/or mass fractions of the reactants) and the properties of the turbulence (in second-order closure). As remarked in the Introduction, consistent with (1) the preliminary character of this investigation, (2) the nature of the formulated model of the mean rate of reactant consumption, and (3) the still imperfect state of second-order closure for turbulent jet flows, in what follows, it is taken that D and B are, at most, specified spatial functions.

III. Approximation for the Mean Velocity Field

With D a specified spatial function, the behavior of the mean velocity field for the jet geometry is governed by

$$U_{,x} + V_{,z} = 0: \quad U = \Psi_{,z}, \quad V = -\Psi_{,x},$$

$$UU_{,x} + VU_{,z} - (DU_{,z})_{,z} = 0$$

$$(0 \le z < \infty, \ 0 \le x < \infty); \qquad (21a)$$

$$U \to 0 \text{ as } z \to \infty, \ V, U_{,z} \to 0 \text{ as } z \to 0; \qquad (21b)$$

$$U \to 1 \text{ for } 0 \le z < z_j = \tfrac{1}{2}\left(\frac{1}{T_j}\right),$$

$$U \to 0 \text{ for } z_j = \tfrac{1}{2}\left(\frac{1}{T_j}\right) < z < \infty$$

$$\text{as } x \to 0. \qquad (21c)$$

Integration of the momentum equation of (21a) with respect to z, subject to the boundary conditions of (21b) and (21c), yields the momentum flux K, an integral flow quantity, defined by

$$K = 2\int_0^\infty U^2\,dz = 2z_j = \left(\frac{1}{T_j}\right). \qquad (22)$$

With the introduction of the 'effective' jet exit plane* x_i (> 0), the 'normal length' function $z_*(x) = z_i(x/x_i)$, with z_i = const., and the 'centerline velocity' function $U_*(x) = u_i(x/x_i)^{-\frac{1}{2}}$, with u_i = const., and with the introduction of (1) the (so-called) similarity coordinates

$$\xi = \left(\frac{x}{x_i}\right), \quad \eta = \frac{z}{z_*(x)} = \left(\frac{x_i}{z_i}\right)\left(\frac{z}{x}\right) = \gamma\left(\frac{z}{x}\right), \qquad (23a)$$

where $\gamma = (x_i/z_i)$ = (constant) spreading parameter (to be determined empirically), and (2) the stream function

$$\Psi(x,z) = \Psi(\xi,\eta) = U_*(\xi)\, z_*(\xi)\, F(\eta)$$

$$= (u_i z_i)\,\xi^{\frac{1}{2}} F(\eta)$$

$$= \frac{1}{\gamma}(u_i x_i)\,\xi^{\frac{1}{2}} F(\eta), \qquad (23b)$$

the velocity components and the vorticity (in the domain $0 \le \eta < \infty$, $1 \le \xi < \infty$) can be written as

$$U = \Psi_{,z} = u_i \xi^{-\frac{1}{2}} F'(\eta),$$

$$V = -\Psi_{,x} = \frac{1}{\gamma} u_i \xi^{-\frac{1}{2}} \left\{\eta F'(\eta) - \tfrac{1}{2} F(\eta)\right\}; \qquad (24a)$$

$$U_{,z} = \Psi_{,zz} = (u_i/z_i)\,\xi^{-3/2} F''(\eta)$$

$$= \gamma(u_i/x_i)\,\xi^{-3/2} F''(\eta). \qquad (24b)$$

Thus, the boundary conditions of (21b) can be written as

$$F'(\infty) = 0, \quad F(0), \quad F''(0) = 0; \qquad (25a)$$

while, by definition,

$$F'(0) = 1. \qquad (25b)$$

In turn, the conservation condition, (22), for momentum takes the form

$$K = 2z_j = \left(\frac{1}{T_j}\right)$$

$$= 2(u_i^2 z_i)\int_0^\infty \left\{F'(\eta)\right\}^2 d\eta$$

$$= \frac{2}{\gamma}(u_i^2 x_i)\int_0^\infty \left\{F'(\eta)\right\}^2 d\eta. \qquad (26)$$

In what follows, an explicit eddy viscosity formulation for D is adopted, namely:

$$D(x,z) = D(\xi) = \kappa\, U_*(\xi)\, z_*(\xi)$$

$$= \kappa(u_i z_i)\xi^{\frac{1}{2}} = \frac{\kappa}{\gamma}(u_i x_i)\xi^{\frac{1}{2}}, \qquad (27)$$

where κ = (constant) eddy-viscosity parameter (to be determined empirically). This form is the one most frequently used in the analysis of two-dimensional jets, because, in general, it has yielded reasonable results (Schlichting[29]). For κ and γ related by $\kappa = 1/(4\gamma)$, the boundary-value problem of (21a) - (21b) reduces to the self-similar form

$$F'''(\eta) + 2\left[F(\eta)F''(\eta) + \left\{F'(\eta)\right\}^2\right] = 0 \ (0 \le \eta < \infty); \qquad (28a)$$

$$F'(\infty) = 0, \quad F(0), \quad F''(0) = 0, \quad F'(0) = 1. \qquad (28b)$$

Successive integrations of (28a) yield

$$F''(\eta) + 2F(\eta)F'(\eta), \ = \text{const.} = 0; \qquad (29a)$$

$$F'(\eta) + \left\{F(\eta)\right\}^2 = \text{const.} = F'(0) = \left\{F(\infty)\right\}^2 = 1. \qquad (29b)$$

Further, (29b), itself, can be integrated to give

*The plane $x = x_i$ (and/or $\xi = 1$) is also referred to as the 'breakpoint'[23] and as the 'flame lift-off distance'.[24]

$F(\eta) = \tanh \eta$:

$$F'(\eta) = 1 - \tanh^2 \eta,$$

$$F''(\eta) = -2 \tanh \eta \, (1 - \tanh^2 \eta). \qquad (30)$$

Based on the solution of (30), it is determined that

$$K = 2z_j = \left(\frac{1}{T_j}\right) = \frac{4}{3}(u_i^2 z_i) = \frac{4}{3\gamma}(u_i^2 x_i). \qquad (31)^*$$

Thus, the solutions for Ψ and U, V are

$$\Psi = \frac{1}{\gamma}(u_i x_i)\xi^{\frac{1}{2}} \tanh \eta$$

$$\approx \left(\frac{3}{4T_j}\right)\xi^{\frac{1}{2}} \tanh \eta \quad \text{for } u_i \approx 1; \qquad (32a)$$

$$U = u_i \xi^{-\frac{1}{2}}(1 - \tanh^2 \eta)$$

$$\approx \xi^{-\frac{1}{2}}(1 - \tanh^2 \eta) \quad \text{for } u_i \approx 1,$$

$$V = \frac{1}{\gamma} u_i \xi^{-\frac{1}{2}} \left\{\eta(1 - \tanh^2 \eta) - \tfrac{1}{2} \tanh \eta\right\}$$

$$\approx \frac{1}{\gamma} \xi^{-\frac{1}{2}} \left\{\eta(1 - \tanh^2 \eta) - \tfrac{1}{2} \tanh \eta\right\}$$

$$\text{for } u_i \approx 1. \qquad (32b)$$

The above solutions to (21a) - (21b) are not the most general ones; they are, in fact, the self-similar solutions for a jet issuing from a slit at $\xi = (x/x_i) = 0$, and, thus, do not satisfy the starting conditions of (21c). In light of the improvement to be expected from alternative, less tractable procedures, it is taken that

$$U \approx \xi^{-\frac{1}{2}}(1 - \tanh^2 \eta)$$

$$= \left(\frac{x}{x_i}\right)^{-\frac{1}{2}} \left(1 - \tanh^2 \left\{\left(\frac{4T_j}{3}\right)\left(\frac{x}{x_i}\right)^{-1} z\right\}\right), \qquad (33a)$$

with

$$U \to \left(\frac{x}{x_i}\right)^{-\frac{1}{2}} \to \infty \quad \text{for } z = 0 \quad \text{as } x \to 0,$$

$$U \to 4\left(\frac{x}{x_i}\right)^{-\frac{1}{2}} \exp\left\{-\left(\frac{8T_j}{3}\right) z \left(\frac{x}{x_i}\right)^{-1}\right\} \to 0$$

$$\text{for } z > 0 \text{ as } x \to 0, \qquad (33b)$$

encompasses the initial conditions of interest for present purposes (i.e., for $x \geq x_i$ and/or $\xi \geq 1$). Thus, (32) furnishes the solution for the jet flow field, with γ an (empirically) assignable parameter.

IV. Rate of Reactant Consumption

With $\sigma_i = \sigma$, the behavior of the (modified) Shvab-Zeldovich function $\overline{Y} = (Y + Y_{O^\infty}) = \left(Y_F + (Y_{O^\infty} - Y_O)\right)$ for the jet geometry is governed by

$$U\overline{Y}_{,x} + V\overline{Y}_{,z} - \frac{1}{\sigma}(D\overline{Y}_{,z})_{,z} = 0$$

$$(0 \leq z < \infty, \; 0 \leq x < \infty); \qquad (34a)$$

$$\overline{Y} \to 0 \text{ as } z \to \infty, \quad \overline{Y}_{,z} \to 0 \text{ as } z \to 0; \qquad (34b)$$

$$\overline{Y} \to (Y_{Fj} + Y_{O^\infty}) \text{ for } 0 \leq z < z_j = \tfrac{1}{2}\left(\frac{1}{T_j}\right),$$

$$\overline{Y} \to 0 \quad \text{for } z_j = \tfrac{1}{2}\left(\frac{1}{T_j}\right) < z < \infty \text{ as } x \to 0. \qquad (34c)$$

The species flux integral associated with this function is

$$N = 2\int_0^\infty U\overline{Y}dz = 2z_j(Y_{Fj} + Y_{O^\infty})$$

$$= \left(\frac{1}{T_j}\right)(Y_{Fj} + Y_{O^\infty}). \qquad (35)$$

In light of the approximations already adopted for the velocity field (cf. (32)), it is taken that $\overline{Y}$ is of the form

$$\overline{Y}(x, z) = \overline{Y}(\xi, \eta) = \overline{Y}_*(\xi)\, G(\eta) = C_i \xi^{-\frac{1}{2}} G(\eta). \qquad (36)$$

With introduction of this form for $\overline{Y}$ and the above-mentioned forms for Ψ and its derivatives, the boundary-value problem of (34a) - (34b) reduces to

$$G''(\eta) + 2\sigma\left[F(\eta)\, G'(\eta) + F'(\eta)\, G(\eta)\right] = 0$$

$$(0 \leq \eta < \infty); \qquad (37a)$$

$$G(\infty) = 0, \quad G'(0) = 0; \qquad (37b)$$

$$G(0) = 1. \qquad (37c)$$

---

* If it is taken that $U(\xi, 0) = U_*(\xi) = u_i \xi^{-\frac{1}{2}}$ for $1 < \xi < \infty$ and that $U(\xi, 0) = 1$ for $0 < \xi < 1$, it is consistent to take $u_i = \left((u_k)_i / u_r\right) = 1$. For $u_i = 1$, from (31), it follows that $z_i = (x_i/\gamma) = (3/4\,T_j)$ and/or $\left((x_k)_i / \ell_r\right) = \left[(3/4)/\left((T_k)_j / T_r\right)\right]\gamma$. Thus, the (non-dimensional) location of the 'effective' jet exit (or 'breakpoint') plane, x_i, is linearly proportional to the jet spreading parameter, γ.

Integration of (37a) yields

$$G'(\eta) + 2\sigma F(\eta)\, G(\eta) = \text{const.} = 0; \qquad (38a)$$

$$G(\eta) = \exp\left\{-2\sigma \int_0^{\eta} F(\eta_1)\, d\eta_1\right\}$$

$$= \left[1 - \left\{F(\eta)\right\}^2\right]^{\sigma} = (1 - \tanh^2\eta)^{\sigma}. \qquad (38b)$$

Based on this solution for G, it follows that the species flux integral N is given by

$$N = 2z_j (Y_{Fj} + Y_{O\infty}) = \left(\frac{1}{T_j}\right)(Y_{Fj} + Y_{O\infty})$$

$$= 2(u_i C_i z_i) \int_0^{\infty} F'(\eta)\, G(\eta)\, d\eta$$

$$= \frac{2}{\gamma}\,(u_i C_i x_i) \int_0^{\infty} F'(\eta)\, G(\eta)\, d\eta$$

$$= \left(\frac{1}{T_j}\right)\left(\frac{C_i}{u_i}\right)\left[\frac{3}{2}\int_0^{\infty} (1 - \tanh^2\eta)^{1+\sigma}\, d\eta\right]. \qquad (39)$$

Thus,

$$C_i = u_i \left(\frac{2}{3I}\right)(Y_{Fj} + Y_{O\infty})$$

$$\approx \left(\frac{2}{3I}\right)(Y_{Fj} + Y_{O\infty}) \quad \text{for } u_i \approx 1, \qquad (40a)$$

where

$$I = I(\sigma) = \int_0^{\infty} (1 - \tanh^2\eta)^{1+\sigma}\, d\eta$$

$$= \int_0^1 (1 - \varphi^2)^{\sigma}\, d\varphi. \qquad (40b)$$

Values of $I(\sigma)$ are: $I(0) = 1$, $I(\frac{1}{2}) = \pi/4$, $I(1) = 2/3$, $I(2) = 8/15$, ... The range of σ of interest is (approximately) $\frac{1}{2} \le \sigma \le 6/5$ (cf. Reynolds[30]). It is noted that, for $\frac{1}{2} \le \sigma \le 1$, $(8/3\pi) \le (2/3I) \le 1$. In what follows, it is taken that $(2/3I) \approx 1$.

Thus, based upon the preceding analysis, the solution for $\overline{Y}$ is of the form

$$\overline{Y} = u_i \left(\frac{2}{3I}\right)(Y_{Fj} + Y_{O\infty})\, \xi^{-\frac{1}{2}} (1 - \tanh^2\eta)^{\sigma}$$

$$\approx (Y_{Fj} + Y_{O\infty})\, \xi^{-\frac{1}{2}} (1 - \tanh^2\eta)^{\sigma},$$

$$\text{i.e., } C_i \approx (Y_{Fj} + Y_{O\infty}),$$

$$\text{for } u_i, \left(\frac{2}{3I}\right) \approx 1. \qquad (41)^*$$

This form is not compatible with the conditions at $\xi = (x/x_i) = 0$. As with the velocity field, it is a self-similar form compatible with a passive scalar issuing from the jet slit at $\xi = (x/x_i) = 0$. Again, in view of the improvement to be expected from alternative, less tractable procedures, it is taken that

$$\overline{Y} \approx (Y_{Fj} + Y_{O\infty}) \cdot$$

$$\left(\frac{x}{x_i}\right)^{-\frac{1}{2}} \left(1 - \tanh^2\left\{\left(\frac{4T_j}{3}\right)\left(\frac{x}{x_i}\right)^{-1} z\right\}\right)^{\sigma} \qquad (42)$$

encompasses the initial conditions of interest for present purposes (i.e., for $x \ge x_i$ and $\xi \ge 1$).

Consider now the behavior of Y_F. With $\sigma_i \ge \sigma$, and with B a specified constant, since $Y_O = Y_{O\infty} - (Y - Y_F)$, the boundary-value problem for Y_F (cf. (12) - (15)) can be written as

$$UY_{F,x} + VY_{F,z} - \frac{1}{\sigma}(DY_{F,z})_{,z}$$

$$= -B\,|U_{,z}|\left[Y_F\left\{Y_{O\infty} - (\overline{Y} - Y_F)\right\}\right]$$

$$(0 \le z < \infty,\ 0 \le x < \infty); \qquad (43a)$$

$$Y_F \to 0 \text{ as } z \to \infty,\ Y_{F,z} \to 0 \text{ as } z \to 0; \qquad (43b)$$

$$Y_F \to Y_{Fj} \text{ for } 0 \le z < z_j = \tfrac{1}{2}\left(\frac{1}{T_j}\right),$$

$$Y_F \to 0 \text{ for } z_j = \tfrac{1}{2}\left(\frac{1}{T_j}\right) < z < \infty \text{ as } x \to 0. \qquad (43c)$$

For Y_F of the form

$$Y_F(x, z) = X(\xi, \eta), \qquad (44)$$

---

*If an effective flame for the turbulent flow is defined by the locus $Y_O = Y_F$, then, $\overline{Y} = Y_{O\infty}$, and

$$\xi_f^{-\frac{1}{2}} (1 - \tanh^2\eta_f)^{\sigma} \approx \frac{Y_{O\infty}}{(Y_{Fj} + Y_{O\infty})}$$

(footnote continued in next column)

(footnote continued from previous column)

gives the shape of the flame. Thus, in the present model, this shape is explicitly a function of Y_{Fj}, $Y_{O\infty}$, and σ only, and is not a function of T_j or $T_\infty (= 1)$. (It should be recalled that all species have been taken to be of comparable molecular weight.) Furthermore, the 'length' of the flame ξ_f^o (with $\xi_f = \xi_f^o$ for $\eta_f = 0$) is given by

$$\xi_f^o \approx \left\{\frac{(Y_{Fj} + Y_{O\infty})}{Y_{O\infty}}\right\}^2.$$

It is seen that the (mean) position of the effective flame, as defined here, is independent of the model adopted for the mean reaction rate $\dot{w}$. The 'thickness' of this effective flame does depend on the model adopted for $\dot{w}$.

from (43), (44) and (32), (41), the boundary-value problem for $X(\xi,\eta)$ in the domain $(0 \le \eta < \infty,\ 1 \le \xi < \infty)$ can be written as

$$X_{,\eta\eta} + 2\sigma\varphi X_{,\eta} - 4\sigma(1-\varphi^2)\xi X_{,\xi} = (8\sigma\gamma B)\left\{\varphi(1-\varphi^2)\right\}\cdot \left[\left\{ Y_{O\infty} - \left[C_i \xi^{-\frac{1}{2}}(1-\varphi^2)^{\sigma} - X\right]\right\}\right],$$

$$\text{with } \varphi = \varphi(\eta) = \tanh\eta; \qquad (45a)$$

$$X \to 0 \text{ as } \eta \to \infty, \quad X_{,\eta} \to 0 \text{ as } \eta \to 0; \qquad (45b)$$

$$X \to X_i = \text{fnc}(\eta) \text{ as } \xi \to 0. \qquad (45c)$$

To complete the formulation of this boundary-value problem for $X(\xi,\eta)$, the profile at the 'effective' jet exit plane $(\xi = 1)$, i.e., $X_i = X_i(\eta)$, must be specified. Here, this initial profile is taken to be

$$X_i = X_i(\eta) = A_i(1-\varphi^2)^{\sigma} = A_i(1-\tanh^2\eta)^{\sigma}, \qquad (46)$$

with A_i = const. (to be specified). For this initial profile for X, it follows that the initial profiles for Y_F and Y_O, i.e., $Y_{Fi}(\eta)$ and $Y_{Oi}(\eta)$, are

$$Y_{Fi} = X_i = A_i(1-\varphi^2)^{\sigma}; \qquad (47a)$$

$$Y_{Oi} = Y_{O\infty} - (\bar{Y}_i - Y_{Fi}) = Y_{O\infty} - (\bar{Y}_i - X_i) = Y_{O\infty} - (C_i - A_i)(1-\varphi^2)^{\sigma}. \qquad (47b)$$

On the centerline at the 'effective' jet exit, $Y_{Fi}(0) = Y^o_{Fi}$ and $Y_{Oi}(0) = Y^o_{Oi}$, with

$$Y^o_{Fi} = A_i, \quad Y^o_{Oi} = Y_{O\infty} - (C_i - A_i). \qquad (48)$$

For $Y^o_{Fi} \approx Y_{Fj}$ and $Y^o_{Oi} \approx 0$, consistent with no combustion upstream of the 'breakpoint',[24] it follows that $A_i \approx Y_{Fj}$ and that $C_i \approx (Y_{Fj} + Y_{O\infty})$ (cf. (41)). Hence, (45c) is taken to be

$$X \to X_i \approx Y_{Fj}(1-\varphi^2)^{\sigma},$$

$$\text{with } \varphi = \varphi(\eta) = \tanh\eta, \text{ as } \xi \to 1. \qquad (45c)'$$

Here, it should be recalled that, in the development of the present model boundary-value problem, (45), there are two empirical factors: γ, the growth rate; and B, the effective Damköhler number. Thus, the model retains the one empirical constant usually present in chemically frozen flow, γ, and adds a second one for the chemistry, B. More specifically, in this model, it is the product γB that is required to characterize the reaction contribution. (With respect to the fluid mechanics, it is noted that the use of, at least, one empirical constant to assign the growth rate is implicitly present in second-order closures, as well.)

With the determination of $Y_F = X$ from (45), the solutions for Y_O and T are determined from

$$Y_O \approx \left[Y_{O\infty}\left\{1 - \xi^{-\frac{1}{2}}(1-\varphi^2)^{\sigma}\right\}\right] - \left[Y_{Fj}\xi^{-\frac{1}{2}}(1-\varphi^2)^{\sigma} - X\right]$$

$$= \left[Y_{O\infty} - (Y_{Fj} + Y_{O\infty})\xi^{-\frac{1}{2}}(1-\varphi^2)^{\sigma}\right] + X; \qquad (49)$$

$$T \approx \left[1 + (T_j - 1)\xi^{-\frac{1}{2}}(1-\varphi^2)^{\sigma}\right] + Q\left[Y_{Fj}\xi^{\frac{1}{2}}(1-\varphi^2)^{\sigma} - X\right]$$

$$= \left[1 + \left\{(T_j - 1) + QY_{Fj}\right\}\xi^{-\frac{1}{2}}(1-\varphi^2)^{\sigma}\right] - QX. \qquad (50)$$

Here, for completeness, it is noted that, as $\xi \to 1$,

$$Y_F \to Y_{Fi} \approx Y_{Fj}(1-\varphi^2)^{\sigma}; \qquad (51a)$$

$$Y_O \to Y_{Oi} \approx Y_{O\infty}\left\{1 - (1-\varphi^2)^{\sigma}\right\}; \qquad (51b)$$

$$T \to T_i \approx 1 + (T_j - 1)(1-\varphi^2)^{\sigma}. \qquad (51c)$$

V. Approximate Solutions - I

Under the transformation

$$(\xi,\eta) \to (\theta,\varphi), \text{ with } \theta = \xi^{-\frac{1}{2}}, \ \varphi = \tanh\eta, \qquad (52)$$

the boundary-value problem for $X = X(\theta,\varphi)$, in the finite domain $(0 \le \theta \le 1,\ 0 \le \varphi \le 1)$ can be rewritten as:

$$(1-\varphi^2)X_{,\varphi\varphi} - 2(1-\sigma)\varphi X_{,\varphi} = -2\sigma\Pi:$$

$$\Pi \approx \theta X_{,\theta} - (4\gamma B)\varphi\left[X\left\{\left[Y_{O\infty}\left(1 - \left\{\theta(1-\varphi^2)^{\sigma}\right\}\right)\right] - \left[Y_{Fj}\left\{\theta(1-\varphi^2)^{\sigma}\right\} - X\right]\right\}\right]; \qquad (53a)$$

$$X \to 0 \text{ as } \varphi \to 1, \quad X_{,\varphi} \to 0 \text{ as } \varphi \to 0; \qquad (53b)$$

$$X \to X_i \approx Y_{Fj}(1-\varphi^2)^{\sigma} \text{ as } \theta \to 1. \qquad (53c)$$

The first and second integrals of (53a), taking into account the boundary conditions of (53b), can be written as

$$X_{,\varphi} = -\frac{2\sigma}{(1-\varphi^2)^{1-\sigma}} \left[\int_0^{\varphi} \frac{\Pi\, d\varphi_1}{(1-\varphi_1^2)^{\sigma}} \right] ; \qquad (54a)$$

$$X = 2\sigma \int_{\varphi}^{1} \left[\int_0^{\varphi_2} \frac{\Pi\, d\varphi_1}{(1-\varphi_1^2)^{\sigma}} \right] \frac{d\varphi_2}{(1-\varphi_2^2)^{1-\sigma}} . \qquad (54b)$$

The value of X at the centerline, $X(\theta, 0) = X^{o}(\theta)$, is, thus,

$$X^{o} = 2\sigma \int_0^{1} \left[\int_0^{\varphi_2} \frac{\Pi\, d\varphi_1}{(1-\varphi_1^2)^{\sigma}} \right] \frac{d\varphi_2}{(1-\varphi_2^2)^{1-\sigma}} . \qquad (54c)$$

To gain approximate solutions, an iteration scheme for the determination of the solution(s) for $X(\theta,\varphi)$ from the integral form(s) of the boundary-value problem, (54), is proposed. To initiate this scheme, it is taken that the zeroth-approximation for $X(\theta,\varphi)$ is of the form

$$X_{(0)}(\theta,\varphi) = X^{o}(\theta)\,(1-\varphi^2)^{\sigma} \approx Y_{Fj} Z(\theta) \left\{ \theta (1-\varphi^2)^{\sigma} \right\} , \qquad (55)$$

with $Z(\theta)$ a function to be determined (subject to the condition that $Z(1) = 1$) (cf. Bush, Feldman and Fendell[9]).

With the introduction of this approximation, evaluation of the integrals of (54c) yields the following (ordinary) differential equation for $Z(\theta)$:

$$\theta Z'(\theta) - \left[(\alpha - \chi\theta) + \lambda \theta Z(\theta) \right] Z(\theta) = 0; \qquad (56a)$$

$$Z(1) = 1 . \qquad (56b)$$

Here,

$$\alpha \approx (2\gamma B)\, I\, Y_{O\infty} \approx (2\gamma B) \left(\frac{2}{3}\right) Y_{O\infty}, \qquad (57a)$$

$$\chi \approx (2\gamma B)\, J\, (Y_{Fj} + Y_{O\infty}), \qquad (57b)$$

$$\lambda \approx (2\gamma B)\, J\, Y_{Fj} , \qquad (57c)$$

where

$$I = I(\sigma) = \int_0^{1} (1-\varphi^2)^{\sigma}\, d\varphi , \qquad (58a)$$

$$J = J(\sigma) = \frac{2\sigma}{1+\sigma} \int_0^{1} \frac{\left[1-(1-\varphi^2)^{1+\sigma} \right]}{(1-\varphi^2)^{1-\sigma}}\, d\varphi . \qquad (58b)$$

The integral $I(\sigma)$ has been introduced previously; the integral $J(\sigma)$, with $J(1) = 7/15$, $J(\frac{1}{2}) = (3\pi - 4)/9$, ..., is introduced here for the first time.

The solution of (56) is determined to be

$$Z(\theta) = \frac{\theta^{\alpha} \exp\left\{\chi(1-\theta)\right\}}{\left[1 + \lambda \int_{\theta}^{1} \theta_1^{\alpha} \exp\left\{\chi(1-\theta_1)\right\} d\theta_1 \right]} . \qquad (59)$$

In turn, with the evaluation of $Z(\theta)$, the first-approximation for $X(\theta,\varphi)$ is found to be

$$X_{(1)}(\theta,\varphi) = X_{(0)}(\theta,\varphi) \left[1 - R_{(1)}(\theta,\varphi) \right] , \qquad (60)$$

where $X_{(0)}(\theta,\varphi)$ is given in (55), and where

$$R_{(1)}(\theta,\varphi) = \alpha \Lambda_I(\varphi) - \left[\chi - \lambda Z(\theta) \right] \theta \Lambda_J(\varphi) . \qquad (61)$$

For $\sigma = 1$,

$$\Lambda_I(\varphi) = \frac{\varphi^2}{1+\varphi} , \qquad (62a)$$

$$\Lambda_J(\varphi) = \frac{\varphi^2}{1+\varphi} - \frac{3}{7}\varphi^3 ; \qquad (62b)$$

while, for $\sigma = \frac{1}{2}$,

$$\Lambda_I(\varphi) = \frac{2}{\pi} \left[\varphi + \frac{(\pi/2)\left\{1-(1-\varphi^2)^{\frac{1}{2}}\right\} - \sin^{-1}\varphi}{(1-\varphi^2)^{\frac{1}{2}}} \right] . \qquad (63a)$$

$$\Lambda_J(\varphi) = \frac{2}{3\pi - 4} \left[\varphi(1-\varphi^2)^{\frac{1}{2}} + 3\, \frac{(\pi/2)\left\{1-(1-\varphi^2)^{\frac{1}{2}}\right\} - \sin^{-1}\varphi}{(1-\varphi^2)^{\frac{1}{2}}} + 2\, \frac{\left\{(1-\varphi^2)^{\frac{1}{2}} - (1-\varphi)\right\}}{(1-\varphi^2)^{\frac{1}{2}}} \right] . \qquad (63b)$$

It is noted that $\Lambda_I(0), \Lambda_J(0) = 0$, such that $R_{(1)}(\theta, 0) = R^{o}_{(1)}(\theta) = 0$. Further, at the 'break-point' plane, $\theta = 1$,

$$R_{(1)}(1,\varphi) = R_{(1)i}(\varphi) = \alpha \Lambda_I(\varphi) - (\chi - \lambda) \Lambda_J(\varphi) \approx (2\gamma B)\, Y_{O\infty} \left[I \Lambda_I(\varphi) - J \Lambda_J(\varphi) \right] \approx \alpha \left[\Lambda_I(\varphi) - \left(\frac{3J}{2}\right) \Lambda_J(\varphi) \right] \qquad (64)$$

Thus, $R_{(1)}(1, 0) = R_{(1)i}(0) = 0$, while, $R_{(1)}(1, 1) = R_{(1)i}(1) \approx f\alpha \neq 0$, with f, a (weak) function of σ, whose numerical value is less than unity. In general, $0 \leq R_{(1)i}(\varphi) \leq f\alpha$, for $0 \leq \varphi \leq 1$.

For $Y_F = Y_F(\theta,\varphi)$ given by

$$Y_F \approx X_{(1)} \approx Y_{Fj}\left[\left\{Z(1-R_{(1)})\right\}\left\{\theta(1-\varphi^2)^\sigma\right\}\right], \quad (65a)$$

then, $Y_O = Y_O(\theta,\varphi)$ is given by

$$Y_O \approx Y_{O\infty} - (\bar{Y} - X_{(1)}) \approx Y_{O\infty}\left[1 - \left\{\theta(1-\varphi^2)^\sigma\right\}\right] - Y_{Fj}\left[\left\{1 - Z(1-R_{(1)})\right\}\left\{\theta(1-\varphi^2)^\sigma\right\}\right]. \quad (65b)$$

To the same order of approximation, $T = T(\theta,\varphi)$ is given by

$$T \approx 1 + \frac{(T_j - 1) + QY_{Fj}}{(Y_{Fj} + Y_{O\infty})}\bar{Y} - QX_{(1)}$$
$$\approx \left[1 + (T_j - 1)\left\{\theta(1-\varphi^2)^\sigma\right\}\right] + QY_{Fj}\left[\left\{1 - Z(1-R_{(1)})\right\}\left\{\theta(1-\varphi^2)^\sigma\right\}\right]$$
$$= \left[1 + \left\{(T_j - 1) + QY_{Fj}\right\}\left\{\theta(1-\varphi^2)^\sigma\right\}\right] - QY_{Fj}\left[\left\{Z(1-R_{(1)})\right\}\left\{\theta(1-\varphi^2)^\sigma\right\}\right]. \quad (66)$$

For $\theta = 1$ (i.e., $\xi = 1$), from (65) and (66), it is determined that

$$Y_{Fi} \approx Y_{Fj}(1-\varphi^2)^\sigma(1 - R_{(1)i}); \quad (67a)$$

$$Y_{Oi} \approx Y_{O\infty}\left\{1 - (1-\varphi^2)^\sigma\right\} - Y_{Fj}(1-\varphi^2)^\sigma R_{(1)i}; \quad (67b)$$

$$T_i \approx 1 + (T_j - 1)(1-\varphi^2)^\sigma + QY_{Fj}(1-\varphi^2)^\sigma R_{(1)i}. \quad (67c)$$

A comparison of (67) and (51) indicates that the original initial conditions are not satisfied exactly by the first iteration solutions.

From (59), it is seen that, as $\theta \to 0$ $(\xi \to \infty)$,

$$Z(\theta) \sim L_0\theta^\alpha\left[1 + O(\theta)\right], \quad (68a)$$

where

$$L_0 = \frac{\exp\lambda}{\left[1 + \lambda\int_0^1 \theta_1^\alpha \exp\left\{\lambda(1-\theta_1)\right\} d\theta_1\right]}. \quad (68b)$$

Thus, the downstream behaviors for Y_F, Y_O, and T, along the centerline, are

$$Y_F^o \sim L_O\theta^{1+\alpha} + \ldots, \quad (69a)$$

$$Y_O^o \sim Y_{O\infty} - (Y_{Fj} + Y_{O\infty})\theta + \ldots; \quad (69b)$$

$$T^o \sim 1 + \left\{(T_j - 1) + QY_{Fj}\right\}\theta + \ldots, \quad (70)$$

where, for explicitness, it is taken that $\left\{(T_j - 1) + QY_{Fj}\right\}$ is a positive quantity. Indeed, based upon (68), it is found that the downstream behaviors for Y_O and T, in general, are

$$Y_O \sim Y_{O\infty} - (Y_{Fj} + Y_{O\infty})\left\{\theta(1-\varphi^2)^\sigma\right\} + \ldots; \quad (71)$$

$$T \sim 1 + \left\{(T_j - 1) + QY_{Fj}\right\}\left\{\theta(1-\varphi^2)^\sigma\right\} + \ldots. \quad (72)$$

With respect to the temperature, it is seen that, downstream, for a fixed value of θ, T is a maximum at $\varphi = 0$ and decreases monotonically as φ increases. Since reaction consumes Y_F, it follows that $Y_F \leq Y_{Fj}\left\{\theta(1-\varphi^2)^\sigma\right\}$, the 'frozen' solution (for $\dot{w} = 0$), and, in turn, that T is augmented (or left the same) when reaction occurs, relative to the nonreacting case. (This result might have been anticipated from (50); here, it follows directly.)

VI. Approximate Solutions - II

A more explicit, but, probably, less accurate, approximate solution of the nonlinear boundary-value of (45) is obtained now through the use of Oseen linearization (Lewis and Carrier[31]; Carrier[32]; Bush, Feldman and Fendell[9]).*

Here, (45a) is approximated by

$$X_{,\eta\eta} + 2\sigma\eta X_{,\eta} - 4\sigma\xi X_{,\xi} \approx (8\sigma\gamma B)(aY_{O\infty}\eta^2)X, \quad (73a)$$

with the constant a considered to be an assignable parameter (that permits the solution of this equation to more adequately approximate that of (45a)). The boundary conditions are those of (45b), i.e.,

---

*In Oseen linearization, terms are approximated in a manner to retain their essential roles, but, also, in a manner to generate analytic tractability. Justification lies entirely in the a posteriori demonstration that, to an adequate degree of accuracy for the purposes in mind, results satisfy the original boundary-value problem.

$$X \to 0 \text{ as } \eta \to \infty, \quad X_{,\eta} \to 0 \text{ as } \eta \to 0. \tag{73b}$$

In lieu of (45c)′, it is required that

$$X \to Y_{Fj} \text{ as } \xi \to 1, \quad \eta \to 0;$$

$$\int_0^\infty X \, d\eta \to Y_{Fj} H \text{ as } \xi \to 1, \tag{73c}$$

where

$$H = H(\sigma) = \int_0^\infty (1 - \tanh^2 \eta)^\sigma \, d\eta = \int_0^1 \frac{d\varphi}{(1-\varphi^2)^{1-\sigma}}. \tag{74}$$

Clearly, $H(\sigma)$ is defined for $\sigma > 0$ only. $H(\frac{1}{2}) = \pi/2$, $H(1) = 1$, $H(3/2) = \pi/4$, $H(2) = 2/3$, ...

On the left-hand side of (73a), the approximations $\tanh \eta \approx \eta$ and $\operatorname{sech} \eta \approx 1$ are employed; while, on the right-hand side, the approximation $\frac{1}{2} |F''(\eta)| Y_O(\xi, \eta) \approx a Y_{O\infty} \eta^2$ is employed. A conventional procedure is to assign the constant a by requiring that the solution to the substitute equation satisfy the original equation in an integral sense over the range of independent variables of interest, i.e., $1 \le \xi < \infty$, $0 \le \eta < \infty$. This procedure is unwieldy in the present case. Here, for explicitness, it is taken that a may be assigned by the equation of $a Y_{O\infty} \eta^2$ to $\frac{1}{2} |F''| Y_O$ at the value of η, for which the latter expression is a maximum. (1) If it is arbitrarily taken that $Y_O \approx Y_{O\infty}$, then, $\frac{1}{2}|F''| = \varphi(1-\varphi^2)$, with $\varphi = \tanh \eta$, is a maximum at $\eta = \tanh^{-1}\{1/\sqrt{3}\}$, and $a \doteq 0.888$. However, such a value for the factor a is too large, because Y_O has been set to its maximum value, a value attained only at large ξ and/or η, where the combustion term is small. (2) If it is taken that $Y_O \approx Y_{Oi} \approx Y_{O\infty}\{1 - (1-\varphi^2)^\sigma\}$ (cf. (51b)), then, a becomes a function of σ, i.e., $a = a(\sigma)$. In fact, the equation of $a\eta^2$ to $\varphi(1-\varphi^2)\{1-(1-\varphi^2)^\sigma\}$ at the value of η for which this latter expression is a maximum yields $a(\frac{1}{2}) \doteq 0.0928$, $a(1) \doteq 0.387$, ... Such values for a are too small, because throughout much, though not all, of that portion of the ξ,η-plane, where the combustion term is appreciable, $Y_O > Y_{Oi}$. However, such estimates suggest the range of interest for values of a for physically pertinent values of the other parameters. Actually, numerical experimentation by the authors indicates that $a(\frac{1}{2}) \doteq 0.28$, $a(1) \doteq 0.48$, ... succeed fairly well. However, the adequacy of these values should be examined in each instance.

Under the transformations

$$\xi^* = \log \xi, \quad \eta^* = (2\sigma)^{\frac{1}{2}} \eta, \tag{75a}$$

$$X(\xi, \eta) = X^*(\xi^*, \eta^*), \tag{75b}$$

(73a) takes the form

$$X^*_{,\eta^*\eta^*} + \eta^* X^*_{,\eta^*} - 2X^*_{,\xi^*} = Q^* \eta^{*2} X^*, \tag{76}$$

with $Q^* = (2\gamma B)(aY_{O\infty}/\sigma) \ge 0$. Solution of this equation is sought of the form

$$X^*(\xi^*, \eta^*) = \sum_{m=0} A^*_m(\xi^*) \eta^{*m} \exp\{-Z^*(\xi^*)\eta^{*2}\}, \tag{77a}$$

with $A^*_m = 0$ for m odd for the case under examination. Here, for simplicity, only the $m = 0$ term is pursued (with $A^*_0(\xi)$, henceforth, denoted by $A^*(\xi^*)$), such that

$$X^*(\xi^*, \eta^*) = A^*(\xi^*) \exp\{-Z^*(\xi^*)\eta^{*2}\}. \tag{77b}$$

This form satisfies (73b). For this form to satisfy (73c), it is determined that

$$A^*(0) = A^*_i = Y_{Fj}; \tag{78a}$$

$$Z^*(0) = Z^*_i = \left\{ \left(\frac{\sqrt{\pi}}{2}\right) \frac{1}{(2\sigma)^{\frac{1}{2}} H} \right\}^2. \tag{78b}$$

Since $H = H(\sigma)$, $Z^*_i = Z^*_i(\sigma)$, with $Z^*_i(\frac{1}{2}) = 1/\pi$, $Z^*_i(1) = \pi/8$, $Z^*_i(3/2) = 4/3\pi$, $Z^*_i(2) = 9\pi/64$, ... $A^*(\xi^*)$ and $Z^*(\xi^*)$, for $\xi^* > 0$, are assigned to satisfy the approximate partial differential equation, (76).

Substitution of (77b) into (76) gives

$$[A^{*\prime} + Z^* A^*] - A^* \eta^{*2} \left[Z^{*\prime}(1 - 2Z^*) - \tfrac{1}{2} Q^* \right] = 0, \tag{79}$$

where primes denote differentiation with respect to ξ^*. Equation of the coefficients of powers of η^* to zero yields

$$Z^{*\prime} - Z^*(1 - 2Z^*) = \tfrac{1}{2} Q^*; \tag{80a}$$

$$A^{*\prime} + Z^* A^* = 0. \tag{80b}$$

The solution for $Z^*(\xi^*)$ is determined to be

$$Z^* = \frac{(S^*+1) - (S^*-1) E^* \exp\{-S^*\xi^*\}}{4\left[1 + E^* \exp\{-S^*\xi^*\}\right]};$$

$$S^* = (1 + 4Q^*)^{\frac{1}{2}} \ge 1;$$

$$E^* = \frac{(S^*+1) - 4Z^*_i}{(S^*-1) + 4Z^*_i}. \tag{81a}$$

Since $(S^*+1) \ge 2$ and since $4/\pi \le Z^*_i \le 9\pi/16 < 2$ for $\frac{1}{2} \le \sigma \le 2$, it follows that $E^* > 0$ (for this range of σ). In turn, it is determined that the solution for $A^*(\xi^*)$ is

$$A^* = A^*_i \exp\left\{-\int_0^{\xi^*} Z^* \cdot d\xi^*_1\right\} = A^*_i \left[\frac{1 + E^*}{1 + E^* \exp\{-S^*\xi^*\}}\right]^{\frac{1}{2}} \exp\left\{-\tfrac{1}{4}(S^*+1)\xi^*\right\}. \tag{81b}$$

Based upon these solutions for Z^* and A^*, it is found that the approximate solution for $X(\xi,\eta)$ takes the form

$$X \approx Y_{Fj}\left(\frac{1+E^*}{\xi^{S^*}+E^*}\right)^{\frac{1}{2}} \xi^{\frac{1}{4}(S^*-1)} \cdot \exp\left\{-\tfrac{1}{2}\sigma\left[\frac{(S^*+1)\xi^{S^*}-(S^*-1)E^*}{\xi^{S^*}+E^*}\right]\eta^2\right\} . \quad (82)$$

As $\xi \to 1$,

$$X \to Y_{Fj} \exp\left\{-\tfrac{1}{2}\sigma(4Z_i^*)\eta^2\right\}, \quad (83a)$$

with Z_i^* given in (78b); while, as $\xi \to \infty$,

$$X \to Y_{Fj}\,\xi^{-\frac{1}{2}(S^*+1)} \exp\left\{-\tfrac{1}{2}\sigma(S^*+1)\eta^2\right\}. \quad (83b)$$

From inspection of this approximate, Gaussian-like form for X, it is noted that the width of the profile decreases with increasing ξ, for fixed η. (This result holds for $(S^*+1) > 4Z_i^*$, i.e., $E^* > 0$.)

For $Q^* = 0$ and/or $S^* = 1$, i.e., for no chemical reaction, the approximate solution of (82) becomes

$$X \approx Y_{Fj}\left(\frac{1+E^*}{\xi+E^*}\right)^{\frac{1}{2}} \exp\left\{-\sigma\left(\frac{\xi}{\xi+E^*}\right)\eta^2\right\}. \quad (84)$$

For this case: as $\xi \to 1$,

$$X \to Y_{Fj} \exp\left\{-\sigma(2Z_i^*)\eta^2\right\}, \quad (85a)$$

just as for the general case; while, as $\xi \to \infty$,

$$X \to Y_{Fj}\,\xi^{-\frac{1}{2}} \exp\{-\sigma\eta^2\}. \quad (85b)$$

The self-similar exact solution for X for the case of no chemical reaction, as calculated from (45) with $B = 0$, is

$$X \approx Y_{Fj}\,\xi^{-\frac{1}{2}}(1-\tanh^2\eta)^{\sigma}. \quad (86)$$

For $\xi \to \infty$, it may be seen that the approximate solution decays appropriately in η as $\eta \to 0$, but too rapidly as $\eta \to \infty$. Still, the general behavior is recovered.

Division of (83b) by (85b) indicates that, for $Q^* > 0$ and/or $S^* > 1$, i.e., for finite chemical reaction, as $\xi \to \infty$,

$$\frac{X_{Q^*>0}}{X_{Q^*=0}} = \frac{X_{S^*>1}}{X_{S^*=1}} \approx \xi^{-\frac{1}{4}(S^*-1)} \exp\left\{-\tfrac{1}{2}\sigma(S^*-1)\eta^2\right\}. \quad (87)$$

Thus, for finite chemical reaction, the fuel profile tends to be of smaller width and magnitude (than for no chemical reaction).

VII. Numerical Solutions

A conventional Crank-Nicolson implicit finite-differencing scheme (cf. Bush, Feldman and Fendell[9]) is employed to obtain numerical solutions to the boundary-value problem of (45). In fact, the program has been written to solve the differential equation

$$X_{,\eta\eta} + 2\sigma\varphi X_{,\eta} - 4\sigma(1-\varphi^2)\xi X_{,\xi} = (8\sigma\gamma B)\left\{\varphi(1-\varphi^2)\right\} \cdot \left[X^m\left\{Y_{O\infty} - \left[C_i\xi^{-\frac{1}{2}}(1-\varphi^2)^{\sigma} - X\right]\right\}^n\right]. \quad (45a)'$$

Clearly, for $m = n = 1$, (45a)′ reduces to (45), i.e., this model with the more generally ordered reaction expression becomes the model treated heretofore. In the scheme used here, three-point differences approximate the derivatives in η (for $0 \le \eta \le 9$), with the step size prespecified and constant (i.e., $\Delta\eta = 0.1$); while, two-point differences approximate the derivatives in ξ (cf. Schlichting[29]). Extrapolation of rates of change in ξ of previous steps establishes the local step size in ξ (except, of course, for the initial step in ξ). The even-symmetry gradient-type condition at the axis is treated (in standard fashion) by the simplest central difference expression. The value of the dependent variable at the one point (external to the field) introduced by this procedure is eliminated by having the differential equation satisfied at the boundary point (Fox[33]). For $m \neq 1$, Taylor series expansions are used to linearize the nonlinear (chemical consumption) term about the nominal local solution for the fuel mass fraction; thus, only a simple inversion of a tridiagonal matrix is required for the linear algebraic equations arising from the finite-differencing. Convergence in η dependence is taken to be effective invariance between successive approximations.

Through numerical integration, using (8a), (23a), and (50), it is readily possible to transform back to x,y-coordinates from ξ,η-coordinates.

It is convenient to characterize results in terms of the integral of the fuel mass fraction, $I_F = I_F(\xi)$, and the normalized integral of the

fuel mass fraction, $\bar{I}_F = \bar{I}_F(\xi) = I_F(\xi)/I_F(1) = I_F/I_{Fi}$, where

$$I_F = \int_0^\infty X\, d\eta; \quad I_{Fi} = \int_0^\infty X_i\, d\eta . \tag{88}$$

Numerically, I_F is obtained by application of Simpson's rule.

VIII. Results

A review of the experimental data on gaseous turbulent fuel jets exhausting into air is useful, before a presentation of the predictions of the present model is given. In this way, the reader may be made aware of what hot-flow measurements are actually available to validate models.

The only data on planar turbulent free-jet diffusion flames (known to the authors) are the very limited measurements due to Kremer,[34] who examined mainly axial behavior for city gas (principally hydrogen and methane) issuing from a 150 mm slot. In 100 slot widths downstream, the axial fuel mole fraction dropped by approximately one-half; while, the axial temperature increased from 100°C to 800°C. A Reynolds number of 3320, based on slot width, produced a fully turbulent flame. Also qualitatively, the spreading of the reacting flow with downstream distance was less than that of an isothermal jet. Kremer recommends use of a turbulent Schmidt number $\sigma \doteqdot 0.75$.* These few statements are about all the data available on planar jet diffusion flames.

Thus, it is necessary to consider experimental results from fuel jets issuing from round orifices, even though one can only qualitatively compare axisymmetric data with planar theory. It may be remarked that Bangert and Roach[36] recently compared predictions (obtained by numerical integration), based on a parabolic reactant-consumption model, very similar to the one proposed here, to the data (for the radial profiles of temperature, fuel mole fraction, oxidant mole fraction, and product mole fraction) furnished, at several downstream positions for an axisymmetric hydrogen fuel jet exhausting into coflowing air, by Kent and Bilger[17] (see, also, Bilger and Beck[18]). Bangert and Roach found that, for $m = n = 1$, $B = 12$ gave uniformly excellent agreement between prediction and experiment for the jet speed/coflowing ambient stream speed ratio ranging from 10 to 2; furthermore, there was rather weak sensitivity to moderate changes in B (say, an increase or decrease in magnitude of 30%) (Bangert, private communication). In particular, the overlapping, coexisting mean profiles for the reactant mass fractions, well known since the results of Hawthorne, Weddell and Hottel,[15] are recovered by the model. Also recovered by the model are (1) the increase and, then, decrease of the axial temperature, (2) the monotonic decrease of the axial fuel mole fraction, and (3) the monotonic increase of the axial oxidant mole fraction, all with increasing downstream distance, as reported by Kent and Bilger. Here, the aim is to point out other experimental evidence that validates the model. Furthermore, the present model is appreciably simpler than that of Bangert and Roach in that (1) it uses a coordinate transformation to correlate the compressible and incompressible equations; (2) it uses an explicit eddy viscosity in preference to a two-equation field-type closure to specify the turbulent diffusion; and (3) it uses a facile self-similar flow field (for a stagnant ambient) in preference to calculating the actual nonself-similar flow field. These appreciable simplifications, previously shown to permit approximate closed-form analytic characterization of the model, are revealed below to sacrifice little in the way of predictive capacity.

For axisymmetric turbulent fuel jets exhausting into stagnant air (for cases of high jet speed and small diameter, such that: the Reynolds number is large, so that molecular processes are negligible relative to inertial effects; and the Froude number is large, so that buoyant accelerations are negligible relative to inertial accelerations), the following experimental results are reported.

1. Reynolds number. Not only is the length of the turbulent flame known to be but weakly a function of the Reynolds number (Hawthorne, Weddell and Hottel[15]), but also the axial temperature distribution is but weakly dependent on the Reynolds number. Kremer[16] states that the number of nozzle diameters downstream at which the maximum temperature occurs is increased by 25%, and that the magnitude of the maximum axial temperature is increased by 15%, when the Reynolds number is increased by a factor of 4.

2. Temperature distribution. At fixed small distances downstream, the maximum temperature occurs several nozzle diameters off the axis (Chigier and Strokin[37]). The radial position of the maximum, and the magnitude of the maximum, first, increase, then, decrease with increasing axial distance downstream. The magnitude of this maximum, with respect to downstream position, rises but slowly after about 10 nozzle diameters downstream; peaks at a value below the adiabatic flame temperature at about that downstream distance at which the maximum goes to the axis (roughly 100 diameters); and, then, decreases appreciably with farther downstream distance (Kremer[16]; Lockwood and Odidi[38]). The temperature on the axis rises monotonically until about

*Kremer's conclusion is based partly on non-reacting flow data; however, for axisymmetric turbulent jet diffusion flames, Eickhoff[35] states: "Compared to the data evaluated for non-reacting jets ..., there seems to be no significant influence of combustion on the ratio of turbulent momentum to mass transport."

100 diameters downstream; then, decreases (Kremer[16]; Guenther and Simon[39]). These remarks concerning the temperature field hold for a coflowing oxidant stream as well, whether that stream be heated (Takeno and Kotani[40]) or not (Kent and Bilger[17]; Bilger and Beck[18]).

3. Flame contour [locus of equal (stoichiometrically adjusted) mass fractions for fuel and oxidant, where, experimentally, an effective composite fuel profile is defined]. As interpreted by Zimont and Meshcheryakov,[41] Kremer[16] finds that the flame contour: first, increases with downstream distance; then, decreases to the axis. However, the flame contour envelopes the maximum temperature contour (i.e., the flame contour lies at a larger radial position at all downstream stations, and goes to the axis farther downstream than does the maximum temperature locus). Measurements of the distance downstream at which the flame contour goes to the axis, i.e., the flame length, are given by Kremer,[16] who found that for other parameters held nearly constant, a city-gas (H_2, CH_4, CO, C_nH_m; N_2, CO_2) turbulent jet diffusion flame is one-and-one-half times as long as a carbon monoxide flame, and a hydrogen flame is two-and-one-quarter times as long. Most other purported measurements are based on visual observations (cf., e.g., Hawthorne, Weddell and Hottel[15]) and are not reported here. Incidentally, Brzustowski[42] finds that published analytic expressions, asserted by their proponents to be *adequate for predicting flame length*, are <u>not</u> adequately verified. This is not unexpected, in that such formulas include unattained quantities, such as the adiabatic flame temperature (e.g., Hawthorne, Weddell and Hottel[15]), or ill-defined quantities, such as the mean flame density (e.g., Beer and Chigier[21]).

4. Species profiles. On the axis, the fuel mass fraction monotonically decreases, while the oxidant mass fraction monotonically increases, with increasing distance downstream. The product mass fractions increase until the fuel is virtually exhausted, and the maximum axial temperature is achieved; then, the product mass fractions decrease with further downstream distance (Kremer[16]; Guenther and Simon[39]). At a fixed downstream station, the fuel mass fraction decreases monotonically and the oxidant mass fraction increases monotonically, with increasing radial distance from the axis. At a shorter downstream distance, the product mass fractions increase to a maximum a few nozzle diameters off the axis; then, decrease. At about the same downstream distance at which the fuel species are effectively totally depleted and the maximum temperature is first achieved on the axis, the maximum of the product mass fractions is also achieved on the axis (Hawthorne, Weddell and Hottel[15]; Kremer[16]; Lavoie and Schlader[43]). These same characterizations hold for a coflowing ambient oxidant stream as well (Kent and Bilger[17]; Bilger and Beck[18]). Chigier and Strokin[37] show that a passive scalar, such as the mass fraction for an inert species, in an axisymmetric turbulent jet diffusion flame employing methane in stagnant air at an exit Reynolds number of 6600, satisfies similarity concepts, in that the passive-scalar field (1) decays (monotonically) axially, with this decay inversely proportional to the first power of the axial distance; (2) decays (monotonically) radially, with this decay a (Gaussian) function of the square of the radial distance/axial distance ratio. The rate of axial decay is about 0.41 times as rapid as that for the nonreacting case.

5. Rate of spread. Turbulent axisymmetric jet diffusion flames have long been known to have a significantly lower rate of spread than a constant-density nonburning jet (Beer and Chigier[21]; Chigier and Strokin[37]). Whereas a nonburning jet may spread at a half-angle of 5-7.5°, a burning jet spreads typically at 2.5-3°. As noted by Zimont and Meshcheryakov,[41] confirmatory evidence is presented by Kremer.[16] In fact, in a related statement, Zimont and Meshcheryakov note that, in a nonreacting jet, the analogous contour for the analogous passive scalar (linear coupling, or Shvab-Zeldovich, function) is uniformly enveloped by the flame contour, and the axial intercept in the nonreacting case is very nearly half the distance downstream that holds for the reacting case. Effectively, then, γ is reduced for the reacting case. Equivalently, x_i is reduced, since x_i and γ are linearly proportional through z_i, i.e., $x_i = z_i\gamma$. (The concept of modifying x_i, in a contractual-mapping-type empirical adjustment, as opposed to modifying γ, in a rate-of-spread-type empirical adjustment, is set forth, for example, by Vulis and Yarin.[44])

6. Velocity Field. Chigier and Strokin[37] and Zimont and Meshcheryakov[41] furnish particularly clear comparisons between nonreacting and reacting jets, for axial decay of the velocity and dynamic pressure. The decay from initial value is reduced in the reacting case.

7. Turbulent diffusion coefficient. Whereas the previously discussed quantities may be directly measured, this quantity must be deduced. Chigier and Strokin[37] and Zimont and Meshcheryakov[41] concur that, axially, the turbulent diffusion coefficient for the reacting case is smaller than that for the nonreacting case for about 10 nozzle diameters downstream; however, by 50 nozzle diameters downstream, the reacting-jet coefficient is twice as large, and, by 100 nozzle diameters, three times as large. Chigier and Strokin[37] also suggest that the turbulent diffusion coefficient decays to one-third its axial value at large radial distances, at distances of 20-30 nozzle diameters downstream.

Attention is now turned from exposition of experimental data to presentation of predictions of the model. First, however, it is noted that, empirically, $\gamma = 7.67$ for the planar nonreacting case (Schlichting[29]); it is known that γ is reduced in

value for the chemically reacting case (Kremer[34]). Here, based upon axisymmetric data, since quantitative planar data are not available, γ is set equal to one-half of its inert value. Second, the specific case chosen for study is a planar turbulent jet of pure carbon monoxide gas at room temperature exhausting into stagnant air, with the reaction taken to proceed by a direct one-step irreversible mechanism to form the product gas carbon dioxide. Accordingly, parametric values are assigned as follows*: $Y_{O\infty} = 0.638$, $Y_{Fj} = 1.56$, $Y_{Oi} = 0$, $T_j = 1$, $Q = 64.4$, and $\gamma = 3.835$. The parameter σ is to be set equal to either $\frac{1}{2}$ or 1; while, γB is to be set equal to 0, 0.1, or 1, for purposes of comparison. Finally, in the expression for mean reactant consumption, the exponent on the fuel mass fraction m is to be set equal to either 1 or 2, for parametric study; while, the exponent on the oxidant mass fraction n is to be set equal to 1. Clearly, the variability in assignment of values for σ, γB, and m reflects uncertainty concerning appropriate values of these parameters.

Some results may be noted prior to the computations. First, for a pure fuel jet exhausting into invitiated air, the flame length $\xi_f^o \approx \{1 + (128\nu_O)/(m_F \nu_F)\}^{\frac{1}{2}}$. For hydrogen, $\nu_O = 1$, $\nu_F = 2$, $m_F = 2$; while, for carbon monoxide, $\nu_O = 1$, $\nu_F = 2$, $m_F = 18$. Thus, the flame length for hydrogen is appreciably longer than that for carbon monoxide, although quantitative comparison is limited by the fact that the approximation of comparable molecular weights for all species has been adopted. In any case, it may be premature to ascribe difficulties in predicting turbulent jet diffusion flame lengths to the neglected role of molecular diffusion (Spalding[13]), as opposed to inadequate modeling of large-scale mixing. Also, since $\xi = x/x_i = (4T_j/3)(x/\gamma)$, it becomes evident that the empirical decrease in γ implies, within the context of the present model, a decrease in the axial decay of the velocity and of a passive scalar (cf. (32b) and (41), respectively). Further, since $\epsilon = DT^2 = (3/16)(4T_j/3)^{\frac{1}{2}}(x/\gamma^3)^{\frac{1}{2}} T^2$, the empirical decrease in γ, but eventual increase in T owing to chemical exothermicity, implies, within the context of the present model, that the turbulent diffusion coefficient for reacting flows is modestly smaller than for frozen flow at small downstream distances, but appreciably larger for large downstream distances. Thus, the present model, for empirically assigned γ, can recover several known trends in the data.

Consideration of the frozen chemistry case, with $B = 0$, permits comparison of the numerical, iterative, and Oseen-linearized solutions with the known exact solutions, for error analysis. For $B = 0$, the mass fractions for fuel and oxidant, individually, are passive scalars, with constant flux integrals (cf. (35)). For $B = 0$, it is expected that $N_1(\xi) = N_2(\xi)$, for $\xi \geq 1$, where

$$N_1(\xi) = \int_0^\infty (1 - \tanh^2 \eta) \cdot X(\xi, \eta)\, d\eta;$$

$$N_2(\xi) = \xi^{-\frac{1}{2}} \int_0^\infty (1 - \tanh^2 \eta) \cdot X(1, \eta)\, d\eta. \qquad (89)$$

The accuracy of the numerical integration is characterized by the results that, for $\sigma = 1$, at $\xi = 15$, $N_1 = 0.2696$, $N_2 = 0.2678$; while, at $\xi = 140$, $N_1 = 0.08886$, $N_2 = 0.08764$. The axial values for the fuel mass fraction, $X(\xi,0) = X^o(\xi)$, found by the iteration scheme are uniformly less than 1% different from (smaller than) those found by the numerical integration, for $1 \leq \xi \leq 140$. The values for $X^o(\xi)$ found by the Oseen-linearization method range between 4% and 11% below those found by the numerical integration, again, for $1 \leq \xi \leq 140$. For $\sigma = \frac{1}{2}$, the flux integrals incur about the same percentage discrepancy as for $\sigma = 1$; however, the axial values found by iteration are uniformly less than 1% too low, while the Oseen-linearization values are up to 20% too high, relative to $X^o(\xi)$ obtained numerically, for $1 \leq \xi \leq 140$. (Clearly, adjusting the Oseen constant a does not avail for $B = 0$, and, in fact, introduction of a second Oseen constant with respect to analytically motivated modifications of the flow field might have been undertaken for purposes of better recovery of the fuel mass fraction field in the frozen case; however, this procedure was not adopted.)

Results for the nominal case, i.e., $\gamma B = 1$, $m = 1$, $n = 1$, $\sigma = \frac{1}{2}$, are plotted in Figs. 2-11. For $\eta = 0$, the monotonic decrease of Y_F (and ρU^2), and the monotonic increase of Y_O, with increasing ξ, are depicted in Fig. 2. The monotonic decrease of Y_F, and the monotonic increase of Y_O, with increasing η, at any fixed $\xi \geq 1$, are depicted in Fig. 3. The maximum temperature occurs off the axis for $\xi < \xi_f^o = 11.82$ (the flame tip distance), but, then, goes to the axis for larger ξ. As seen in Fig. 4, the magnitude of the maximum temperature increases with increasing ξ for $\xi < \xi_f^o$, though most of the increase occurs at relatively small ξ; then, this magnitude decreases for $\xi > \xi_f^o$. These results are amplified in Fig. 5, where it is shown that, at given ξ, the y-position of the locus $Y_O = Y_F = X_f$ increases, then, decreases, with increasing ξ, but, nevertheless, always exceeds the y-position of the maximum temperature. All these results are compatible in trend with experimental data, discussed earlier, and are of plausible magnitude, when allowance is made for the planar geometry. Whereas Figs. 2-5 involve the numerical solutions only, Figs. 6-10

*It is recalled that $Y_O = (m Y_O^+)/(m_O \nu_O)$, $Y_F = (m Y_f^+)/(m_F \nu_F)$, where $m = m_O \nu_O + m_F \nu_F$, and Y_i^+ is the mass fraction of species i.

indicate the adequacy of the approximate methods of solution. (Here, for $\sigma = \frac{1}{2}$, the Oseen-linearization constant a is set equal to 0.38, as opposed to the 0.28 value suggested earlier after numerical experimentation.) Fig. 11 reveals that, in the conservation equation for fuel, turbulent diffusion and tangential (streamwise) convection balance near the axis, but normal convection and chemical reaction (consumption) play a significant role off the axis; at large distances from the axis, diffusion and normal convection dominate. It seems worth noting that plausible profiles are generated by a model that uniformly permits no consumption on the axis.

In Table 1, numerical results for the nominal case are compared with numerical results obtained from the model by sequentially altering one parameter at a time. Increasing the turbulent Schmidt number increases the axial values of the fuel mass fraction and the distance off axis of the flame. Increasing the fuel or oxidant exponent in the consumption term decreases the amount of fuel consumption; while, increasing the effective turbulent Damköhler number γB increases the amount of fuel consumption. (By numerical experimentation for the case of $\gamma B = \sigma = m = n = 1$, in the Oseen-linearization model, $a = 0.62$, as opposed to $a = 0.48$, mentioned above, gives closest agreement with the results from the finite-difference integration; in fact, the axial fuel mass fraction is missed, i.e., over estimated, by less than 1%, for $1 \leq \xi \leq 30$.)

In conclusion, the authors feel that, in the present paper, the following have been demonstrated: (1) the postulated model captures the essential physics (i.e., the experimental results) for the turbulent portion of the planar fuel jet; and (2) the given approximate solutions capture the essence of the model. It is suggested that studies of other parametric cases may be made using the approximate solutions, rather than the numerical solutions.

References

[1] Kerber, R. L., Emanuel, G. and Whittier, J. S., "Computer Modeling and Parametric Study of a Pulsed $H_2 + F_2$ Laser," Appl. Optics, Vol. 11, pp. 1112-1123.

[2] Davies, P. O. A. L. and Yule, A. J., "Coherent Structures in Turbulence," J. Fluid Mech., Vol. 69, 1975, pp. 513-537.

[3] Roshko, A., "Structure of Turbulent Shear Flows: A New Look," AIAA J., Vol. 14, 1976, pp. 1349-1357.

[4] Bush, W. B. and Fendell, F. E., "Diffusion-flame Structure for a Two-step Chain Reaction," J. Fluid Mech., Vol. 68, 1974, pp. 701-724.

[5] Carrier, G. F., Fendell, F. E. and Marble, F. E., "The Effect of Strain Rate on Diffusion Flames," SIAM J. Appl. Math., Vol. 28, 1975, pp. 463-500.

[6] Carrier, G. F. and Fendell, F. E., "The Effect of Strain Rate on Diffusion Flames. II. Large Straining," SIAM J. Appl. Math., Vol. 30, 1976, pp. 515-527.

Table 1. Calculated Results

Case (γB, σ, m, n)	$\xi = 3$				$\xi = 8$				$\xi = \xi_f^o = 11.821$	
	X^o	$\bar{I}_F$	X_f	η_f	X^o	$\bar{I}_F$	X_f	η_f	$X^o = X_f^o$	$\bar{I}_F$
Nominal (1, $\frac{1}{2}$, 1, 1)	0.787	0.461	0.346	1.31	0.388	0.224	0.298	0.645	0.288	0.165
$\sigma = 1$ (1, 1, 1, 1)	0.798	0.458	0.339	0.876	0.399	0.224	0.305	0.449	0.298	0.166
m = 2 (1, $\frac{1}{2}$, 2, 1)	0.803	0.495	0.381	1.31	0.439	0.275	0.353	0.645	0.348	0.218
$\gamma B = 1.8$ (1.8, $\frac{1}{2}$, 1, 1)	0.740	0.414	0.302	1.31	0.332	0.180	0.246	0.645	0.234	0.125
n = 2 (1, $\frac{1}{2}$, 1, 2)	0.862	0.529	0.406	1.31	0.478	0.289	0.380	0.645	0.373	0.225

Notes:
(1) $Y_F(\xi, 0; \ldots) = X^o(\xi; \ldots)$ is denoted above by $X^o(\xi)$.
(2) $\bar{I}_F(\xi;\sigma) = I_F(\xi;\sigma)/I_F(1;\sigma) = I_F(\xi;\sigma)/I_{Fi}(\sigma)$ is denoted above by $\bar{I}_F(\xi)$; $I_{Fi}(\frac{1}{2}) = 2.44$, $I_{Fi}(1) = 1.56$.
(3) $X(\xi, \eta_f; \ldots) = X_f(\xi; \ldots)$ is denoted above by $X_f(\xi)$, with $\eta_f(\xi;\sigma)$ denoted by $\eta_f(\xi)$.

[7]Bush, W. B. and Fendell, F. E., "On Diffusion Flames in Turbulent Shear Flows," Acta Astro., Vol. 1, 1974, pp. 645-666.

[8]Bush, W. B. and Fendell, F. E., "On Diffusion Flames in Turbulent Shear Flows: The Two-step Symmetrical Chain Reaction," Combustion Sci. and Tech., Vol. 11, 1975, pp. 35-48.

[9]Bush, W. B., Feldman, P. S. and Fendell, F. E., "On Diffusion Flames in Turbulent Shear Flows: Modeling Reactant Consumption in a Mixing Layer," Combustion Sci. and Tech., Vol. 13, 1976, pp. 27-54.

[10]Spalding, D. B., "Mixing and Chemical Reaction in Steady Confined Turbulent Flames," Thirteenth Symposium (International) on Combustion, Combustion Institute, Pittsburgh, Penn., 1971, pp. 649-657.

[11]Spalding, D. B., "Concentration Fluctuations in a Round Turbulent Free Jet," Chem. Eng. Sci., Vol. 26, pp. 95-107.

[12]Ooms, G. and Wicks, M., "Concentration Fluctuations in a Turbulent Jet," Appl. Sci. Res., Vol. 30, 1975, pp. 381-399.

[13]Spalding, D. B., "Mathematical Models of Turbulent Flames: A Review," Combustion Sci. and Tech., Vol. 13, 1976, pp. 3-25.

[14]Reynolds, W. C., "Computation of Turbulent Flows," Annual Review of Fluid Mechanics, Vol. 8 (Eds. M. van Dyke, W. G. Vincenti, and J. V. Wehausen), Annual Reviews, Stanford, Calif., 1976, pp. 183-208.

[15]Hawthorne, W. R., Weddell, D. S. and Hottel, H. C., "Mixing and Combustion in Turbulent Gas Jets," Third Symposium on Combustion, Flame and Explosion Phenomena, Williams and Wilkins, Baltimore, Maryland, 1949, pp. 266-288.

[16]Kremer, H., "Strömung und Mischung in frei brennenden Diffusionsflammen," VDI-Berichte Nr. 95, VDI-Verlag, Dusseldorf, Germany, 1966, pp. 55-69.

[17]Kent, J. H. and Bilger, R. W., "Turbulent Diffusion Flames," Fourteenth Symposium (International) on Combustion, Combustion Institute, Pittsburgh, Penn., 1973, pp. 615-625.

[18]Bilger, R. W. and Beck, R. E., "Further Experiments on Turbulent Jet Diffusion Flames," Fifteenth Symposium (International) on Combustion, Combustion Institute, Pittsburgh, Penn., 1975, pp. 541-552.

[19]Williams, F. A., "Comments on the Theories and Suggestions for the Experimentalists," Combustion Sci. and Tech., Vol. 13, 1976, pp. 251-253.

[20]Grohs, G. L., "Chemical Laser Cavity Mixing and Turbulence," AIAA Paper 76-56, AIAA, New York, N. Y., 1976, 12pp.

[21]Beer, J. M. and Chigier, N. A., Combustion Aerodynamics, John Wiley, New York, N. Y., 1972.

[22]Davies, J. T., Turbulence Phenomena, Academic Press, New York, N. Y., 1972.

[23]Lessen, M. and Paillet, F., "Marginal Instability of Turbulent Shearing Layers and the Break Point of a Jet," Phys. Fluids, Vol. 19, 1976, pp. 943-944.

[24]Wohl, K. and Shipman, C. W., "Diffusion Flames," Combustion Processes (High Speed Aerodynamics and Jet Propulsion, Vol. 2) (Eds. B. Lewis, R. N. Pease, and H. S. Taylor), Princeton University Press, Princeton, N. J., 1956, pp. 365-404.

[25]Tamanini, F., "Numerical Model for the Prediction of Buoyancy Controlled, Turbulent Diffusion Flames (A Description of the FUELJET2 Computer Program)," Factory Mutual Research, Basic Research Dept. Tech. Rept. 22360-1, Norwood, Mass., 1975, 93pp. and apps.

[26]Gutmark, E. and Wygnanski, I., "The Planar Turbulent Jet," J. Fluid Mech., Vol. 73, 1976, pp. 465-495.

[27]Kotsovinos, N. E., "A Note on the Spreading Rate and Virtual Origin of a Plane Turbulent Jet," J. Fluid Mech., Vol. 77, 1976, pp. 305-311.

[28]Batt, R. G., "Experimental Investigation of the Effect of Shear Flow Turbulence on a Chemical Reaction," TRW Systems, Engineering Sciences Lab. Rept., Redondo Beach, Calif., 1974, 101pp.

[29]Schlichting, H., Boundary-Layer Theory (6th Ed.), McGraw-Hill, New York, N. Y., 1968, pp. 696-698.

[30]Reynolds, A. J., "The Variation of Turbulent Prandtl and Schmidt Numbers in Wakes and Jets," Int. J. Heat and Mass Transf., Vol. 19, 1976, pp. 757-764.

[31]Lewis, J. A. and Carrier, G. F., "Some Remarks on the Flat Plate Boundary Layer," Quart. Appl. Math., Vol. 7, 1949, pp. 228-234.

[32]Carrier, G. F., "Analytic Approximation Techniques in Applied Mathematics," J. Soc. Indust. Appl. Math., Vol. 13, 1965, pp. 68-95.

[33] Fox, L., "Parabolic Equations in Two Dimensions: II," Numerical Solution of Ordinary and Partial Differential Equations (Ed. L. Fox), Pergamon Press, Oxford, Eng., 1962, pp. 242-254.

[34] Kremer, H., "Mixing in a Plane Free-Turbulent-Jet Diffusion Flame," Eleventh Symposium (International) on Combustion, Combustion Institute, Pittsburgh, Penn., 1967, pp. 799-806.

[35] Eickhoff, H. E., "Experimental Investigation of the Influence of Combustion on Turbulent Transport in Jet Diffusion Flames," Combustion Institute European Symposium (Ed. F. Weinberg), Academic Press, New York, N. Y., 1973, pp. 513-517.

[36] Bangert, L. H. and Roach, R. L., "Study of Effects of Injector Geometry on Fuel-Air Mixing and Combustion," Georgia Inst. of Tech., School of Aerospace Eng'ng. Prog. Rept., Atlanta, Ga., 1976, 48 pp.

[37] Chigier, N. A. and Strokin, V., "Mixing Processes in a Free Turbulent Diffusion Flame," Combustion Sci. and Tech., Vol. 9, 1974, pp. 111-118.

[38] Lockwood, F. C. and Odidi, A. O. O., "Measurement of Mean and Fluctuating Temperature and of Ion Concentration in Round Free-Jet Turbulent Diffusion and Premixed Flames," Fifteenth Symposium (International) on Combustion, Combustion Institute, Pittsburgh, Penn., 1975, pp. 561-571.

[39] Guenther, R. and Simon, H., "Turbulence Intensity, Spectral Density Functions, and Eulerian Scales of Emission in Turbulent Diffusion Flames," Twelfth Symposium (International) on Combustion, Combustion Institute, Pittsburgh, Penn., 1969, pp. 1069-1079.

[40] Takeno, T. and Kotani, Y., "A Study of the Structure of Turbulent Jet Diffusion Flames," Combustion Sci. and Tech., Vol. 10, 1975, pp. 45-57.

[41] Zimont, V. L. and Meshcheryakov, E. A., "Integral-Method Calculation of Turbulent Diffusion Combustion of a Jet in an Oxidant Volume and of a Jet with Primary Oxidant Entrainment with Concentration Fluctuations Taken into Account," Combustion, Explosion, and Shock Waves, Vol. 10, 1975, pp. 190-197.

[42] Brzustowski, T. A., "A New Criterion for the Length of a Gaseous Diffusion Flame," Combustion Sci. and Tech., Vol. 6, 1973, pp. 313-319.

[43] Lavoie, G. A. and Schlader, A. F., "A Scaling Study of NO Formation in Turbulent Diffusion Flames of Hydrogen Burning in Air," Combustion Sci. and Tech., Vol. 8, 1974, pp. 215-224.

[44] Vulis, L. A. and Yarin, L. P., "Calculated Structure of a Diffusion Flame," Combustion, Explosion, and Shock Waves, Vol. 10, 1975, pp. 131-139.

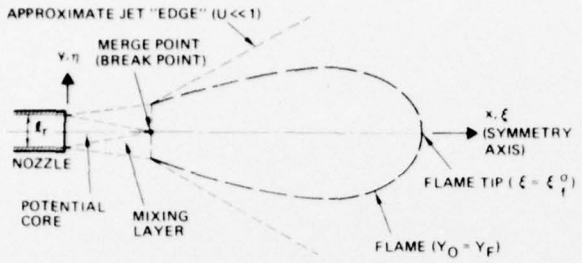

Fig. 1. Schematic diagram, not to scale, of a lifted subsonic planar turbulent fuel jet exhausting into a stagnant oxidant-containing ambient, with the flame locus defined by the condition of equal values for the (stoichiometrically adjusted) mass fraction for fuel, Y_F, and for oxidant, Y_O. At the axis of symmetry $y = \eta = 0$; x, ξ are streamwise coordinates.

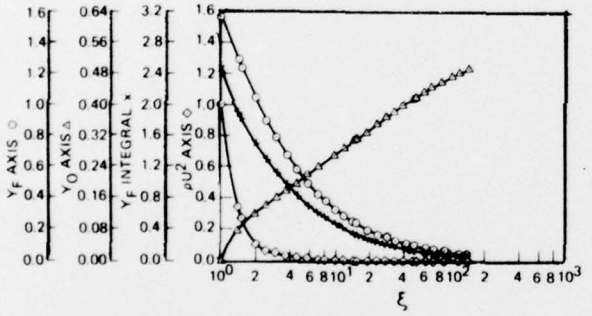

Fig. 2. For the nominal case (Y_{O_∞} = 0.638, Y_{F_j} = 1.56, $Y^\circ_{O_i}$ = 0, T_j = 1, Q = 64.4, γ = 3.835, $B\gamma$ = 1, σ = 0.5, m = n = 1), the following quantities are plotted against the streamwise similarity coordinate ξ, from the break point ξ = 1: the axial fuel mass fraction, $Y_F(\xi,0)$; the axial oxidant mass fraction, $Y_O(\xi,0)$; the integral of $Y_F(\xi,\eta)$ over the transverse similarity coordinate η, $I_F(\xi)$; and the axial dynamic pressure, $\rho(\xi,0)\cdot U^2(\xi,0)$.

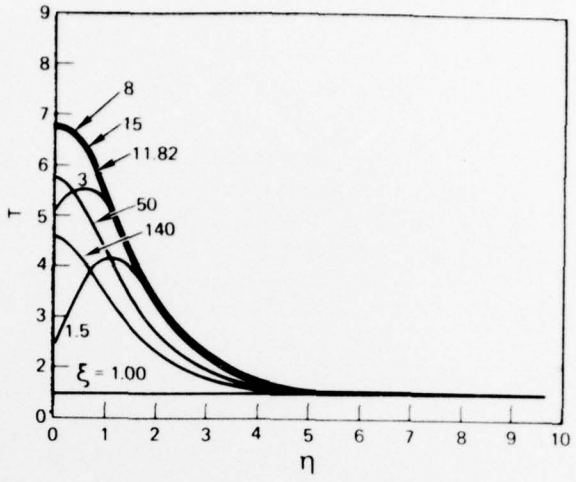

Fig. 3. For the nominal case, the static temperature $T(\xi,\eta)$ is given as a function of the (density-scaled) transverse similarity coordinate η, at several values of the streamwise similarity coordinate ξ, where $\xi = \xi^\circ_f = 11.82$ is the flame tip $[Y_F(\xi^\circ_f, 0) = Y_O(\xi^\circ_f, 0)]$.

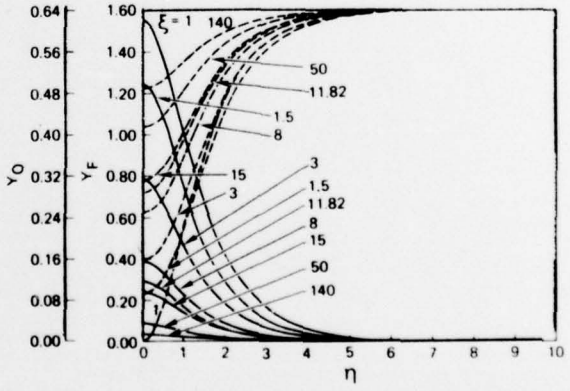

Fig. 4. For the nominal case, the fuel mass fraction Y_F (solid curves) and the oxidant mass fraction Y_O (dashed curves) are given as a function of the transverse similarity coordinate η, at several values of the streamwise similarity coordinate ξ.

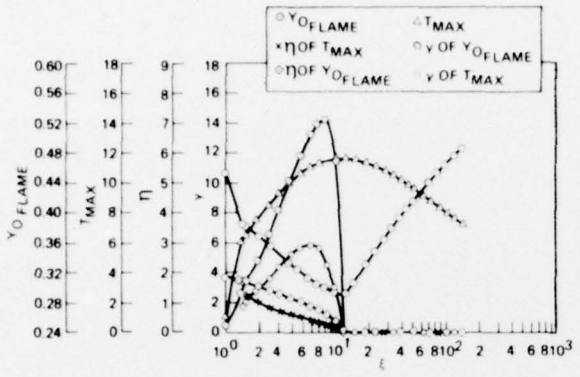

Fig. 5. For the nominal case, the following quantities are given as a function of the streamwise similarity coordinate ξ, for $\xi \geq 1$ (where $\xi = 1$ is the break point): the value of $Y_0 (= Y_F)$ at the flame locus for $\xi \leq 11.82$ (where $\xi = 11.82$ is the flame tip position), this curve giving the axial value of the oxidant mass fraction $Y_0(\xi,0)$ for $\xi \geq 11.82$; the value of η at which $Y_0 = Y_F$ for given ξ; the equivalent value of y at which $Y_0 = Y_F$ for given ξ; the maximum value of the static temperature T at any η for given ξ, T_{MAX}; the value of η at which T_{MAX} occurs for given ξ; and the equivalent value of y at which T_{MAX} occurs for given ξ.

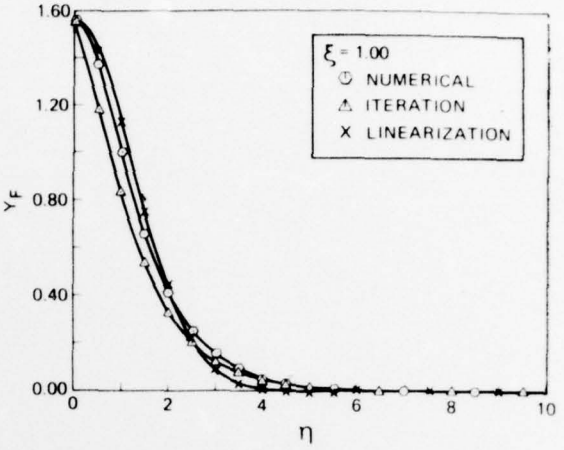

Fig. 6. For the nominal case, a comparison of the fuel mass fraction profiles Y_F over transverse similarity coordinate η, for $\xi = 1$ (the break point), as obtained by numerical integration, by iteration, and by Oseen linearization (a = 0.38).

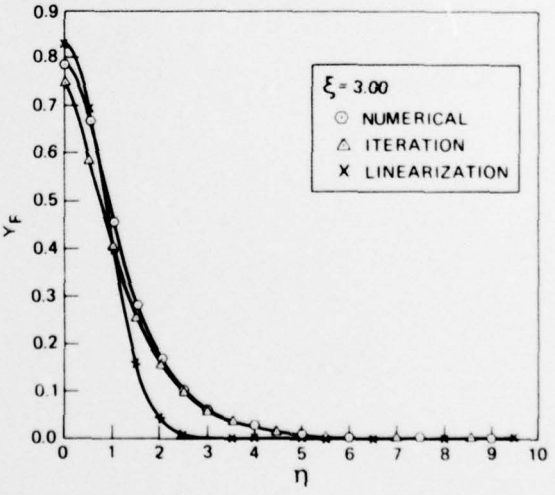

Fig. 7. Analogous plot to Fig. 6, for $\xi = 3.0$.

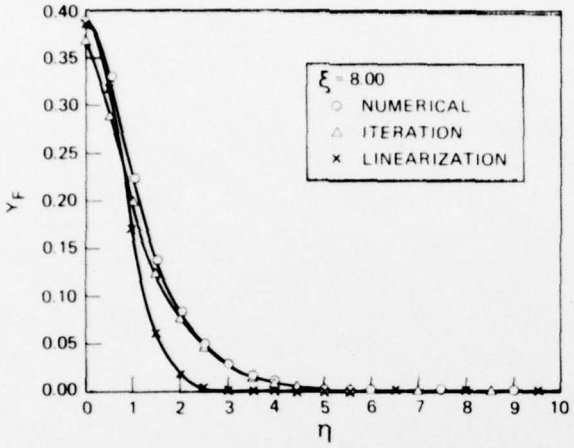

Fig. 8. Analogous plot to Fig. 6, for $\xi = 8.0$.

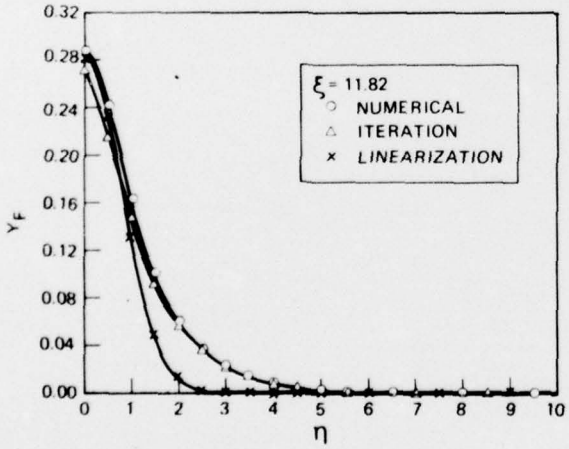

Fig. 9. Analogous plot to Fig. 6, for $\xi = 11.82$ (the flame tip position).

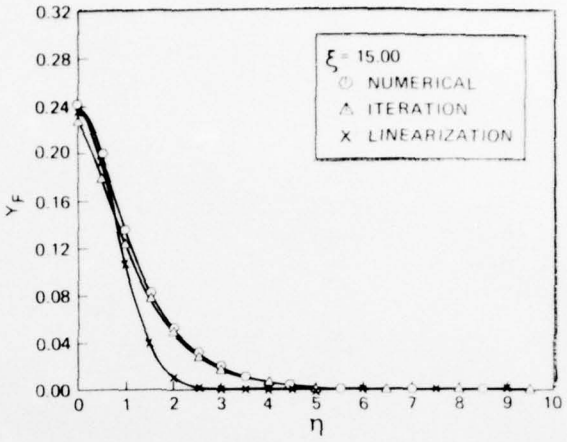

Fig. 10. Analogous plot to Fig. 6, for $\xi = 15.0$.

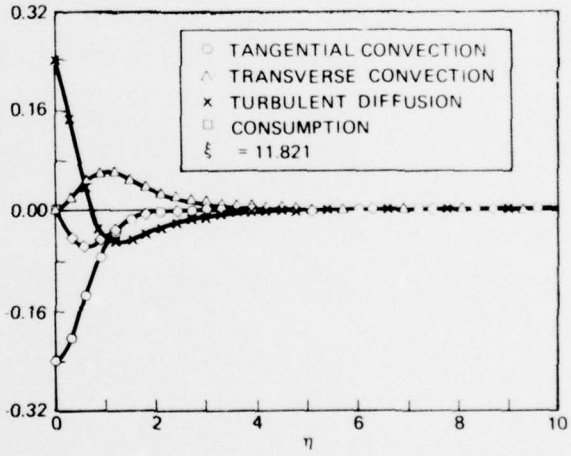

Fig. 11. For the nominal case, at the distance downstream of the flame tip $\xi = 11.82$, the values of the terms comprising the model mean equation of conservation of the fuel species [tangential (streamwise) convection, transverse convection, turbulent diffusion, and consumption (chemical reaction)] are given as a function of the transverse similarity coordinate η.